

LAMINAR BURNING VELOCITY OF ISOCTANE-AIR,
METHANE-AIR, AND METHANOL-AIR MIXTURES AT HIGH
TEMPERATURE AND PRESSURE

by

Mohamad Metghalchi

B. S. University of Oklahoma
(1975)

SUBMITTED IN PARTIAL FULFILLMANT OF THE
REQUIREMENTS FOR THE DEGREE OF
MASTER OF SCIENCE

at the

MASSACHUSETTS INSTITUTE OF TECHNOLOGY

October, 1976

(10-5-1976) (1977)

Signature of Author

Department of Mechanical Engineering, October 29 1976

Certified by

Accepted by

Chairman, Departmental Committee on Graduate Students



LAMINAR BURNING VELOCITY OF ISOCTANE-AIR,
METHANE-AIR, AND METHANOL-AIR MIXTURES AT HIGH
TEMPERATURE AND PRESSURE

by

Mohamad Metghalchi

Submitted to the Department of Mechanical Engineering on October 29, 1976,
in partial fulfillment of the requirements for the degree of Master of
Science.

ABSTRACT

A spherical combustion bomb was constructed to perform laminar burning velocity measurements for different fuels. A thermodynamic analysis is used to calculate laminar burning velocity from a pressure time trace of the combustion process. The state of the burned gases were determined using an equilibrium program. Ionization probes are used to assure that spherical symmetry exists.

The laminar burning velocities of methane-air mixtures were measured in the range of 1 to 50 ATM pressure and temperature of 300 to 550 °k. For isooctane-air burning velocities were measured in the range of 1 to 25 ATM pressure and temperature of 300 to 550 °k and for methanol-air mixture laminar burning velocities were measured for pressures between 1 to 15 ATM and temperature of 300 to 550 °k.

Thesis Supervisor: James C. Keck
Title: Ford Professor of Engineering

ACKNOWLEDGMENTS

The author wished to express his gratitude to Professor J. C. Keck, his Thesis Advisor, for the opportunity to do this work and especially for his valuable advice and suggestions during the preparation of this thesis. The author would like to express his appreciation to Dr. D. Appel, Mr. C. Ferguson, and Mr. F. Yee for their assistance.

The author also would like to thank Ms. M. Pericola for her excellent typing of the final draft. Finally, I wish to dedicate this work to my parents whose helpful support and guidance through my entire academic career stimulated and encouraged me towards completion.

TABLE OF CONTENTS

	<u>Page</u>
TITLE PAGE	1
ABSTRACT	2
ACKNOWLEDGMENTS	3
TABLE OF CONTENTS	4
LIST OF TABLES	6
LIST OF FIGURES	7
1.0 INTRODUCTION	10
2.0 REVIEW OF MEASURING TECHNIQUE AND ANALYSIS	13
2.1 Analysis of Constant Volume Spherical Bomb Combustion	14
2.1.1 Flow Effects.	14
2.1.2 Burning Velocity Determination From the Pressure Record.	16
3.0 EXPERIMENTAL APPARATUS.	19
3.1 Combustion Bomb.	19
3.2 Spark Plugs and Electrodes	19
3.3 Ionization Probes.	20
3.4 Data Collection	20
4.0 ANALYSIS OF PRESSURE-TIME DATA.	22
5.0 DISCUSSION OF RESULTS	27
5.1 Parametric Fit of Measured Burning Velocities	27
5.2 Methane-Air Mixture.	30

TABLE OF CONTENTS (Cont.)

	<u>Page</u>
5.3 Comparison of Values of Burning Velocity for Methane-Air Mixture	32
5.4 Isooctane-Air Mixture	33
5.5 Comparison of Values of Burning Velocity for Isooctane-Air Mixture	36
5.6 Methanol-Air Mixture	36
5.7 Comparison of Values of Burning Velocity for Methanol-Air Mixture	39
6.0 CONCLUSION AND SUGGESTIONS	40
APPENDIX I BURNING VELOCITY FIT AND ERROR ANALYSIS	42
APPENDIX II ANALOG DIFFERENTIATOR AND CORRESPONDING ANALYSIS.	49
REFERENCES	54
TABLES	57
FIGURES	60

LIST OF TABLES

<u>Tables</u>		<u>Page</u>
1	S_{uo} , α , β , ϵ , and Their R.M.S. Errors For Methane-Air Mixtures at Equivalence Ratios of 0.8, 1.0, and 1.2.	30
2	S_{uo} , α , β , ϵ , and Their R.M.S. Errors for Isooctane-Air Mixtures at Equivalence Ratios of 0.8, 1.0, and 1.2.	34
3	S_{uo} , α , β , ϵ , and Their R.M.S. Errors For Methanol-Air Mixtures at Equivalence Ratios of 0.8, 1.0, and 1.2.	37
4	S_{uo} , α , β , ϵ , and Their R.M.S. Errors for Methane-Air Mixtures at Equivalence Ratio Ranging from 0.8 to 1.3.	57
5	S_{uo} , α , β , ϵ , and Their R.M.S. Errors for Isooctane-Air Mixtures at Equivalence Ratio Ranging from 0.7 to 1.6.	58
6	S_{uo} , α , β , ϵ , and Their R.M.S. Errors For Methonal-Air Mixtures at Equivalence Ratio Ranging from 0.7 to 1.5.	59

LIST OF FIGURES

<u>Figure</u>		<u>Page</u>
1	Particle Trajectories of Stoichiometric Methane-Air Mixture with Initial Conditions of $P_i = 1$ ATM and $T_i = 300^\circ\text{k}$ Having Constant Burning Velocity ($S_u = \text{Const.} = 1$).	60
2	Flame Speed Versus Burning Velocity for Stoichiometric Methane-Air Mixture with Initial Condition of $P_i = 1$ ATM and $T_i = 300^\circ\text{k}$.	61
3	Comparison of Burning Velocity Equations .	62
4	Schematic Diagram of the Combustion Bomb (Third Ionization Gage Port is Behind Valve Port)	63
5	Schematic Diagrams Showing Construction of Ionization Probes.	64
6	Schematic Diagrams of Ionization Probe Circuit.	65
7	Schematic Diagram of Experimental Apparatus .	66
8	Ideal Pressure-Time Diagram and Ionization Probe Signals. Horizontal Curves: Ionization Probe Signals, and the Other Curve: Pressure-Time Diagram.	67
9	Pressure-Time Diagram and Ionization Probe Signals If Air-Fuel Mixture is not Homogeneous or the Electrodes are not at the Center of the Combustion Bomb.	67
10	Oscillogram for Methane-Air Mixture at Equivalence Ratio of 0.9 and Initial Condition of $P_i = 1$ ATM and $T_i = 300^\circ\text{k}$ (Vertical Scale is 1.36 ATM/DIV., and t Horizontal Scale is 10 MSEC/DIV.).	68
11	Measured and Fitted Burning Velocity of Methane-Air Mixtures at Equivalence Ratio of 0.8, 1.0, and 1.2 with Initial Temperature of 300°k and Four Different Initial Pressure of 1, 2.04, 3.06, and 4.08 ATM (Point "p" Represents Point of Discontinuity of Ionization Probes.)	69

LIST OF FIGURES (Cont.)

<u>Figure</u>		<u>Page</u>
12	Measured and Fitted Burning Velocity of Isooctane-Air Mixtures with Initial Temperature of 300°k and Initial Pressure of 1 ATM with Equivalence Ratio Ranging from 0.7 to 1.6. (Point "p" Represents Point of Discontinuity of Ionization Probes).	70
13	Measured and Fitted Burning Velocity of Methanol-Air Mixtures with Initial Temperature of 300°k and Initial Pressure of 1 ATM with Equivalence Ratio Ranging from 0.7 to 1.5. (Point "p" Represents Point of Discontinuity of Ionization Probes.)	71
14	S_{uo} as a Function of Equivalence Ratio for Methane-Air Mixtures ($T_o = 300^\circ\text{k}$, $P_o = 1 \text{ ATM}$), Errors are Shown and the Curve is the Least Square Fit of 4th Order Polynomial.	72
15	Contour Plot of Burning Velocity, Unburned Gas Temperature, and Normalized Unburned Density for Methane-Air Mixture at Equivalence Ratio of 0.8 ($P_o = 1 \text{ ATM}$, $T_o = 300^\circ\text{k}$).	73
16	Contour Plot of Burning Velocity, Unburned Gas Temperature, and Normalized Unburned Density for Stoichiometric Methane-Air Mixture ($P_o = 1 \text{ ATM}$, $T_o = 300^\circ\text{k}$).	74
17	Contour Plot of Burning Velocity, Unburned Gas Temperature, and Normalized Unburned Density for Methane-Air Mixture at Equivalence Ratio of 1.2 ($P_o = 1 \text{ ATM}$, $T_o = 300^\circ\text{k}$).	75
18	Burning Velocity for Isentropes of Methane-Air Mixtures at Different Equivalence Ratio ϕ as a Function of Pressure with Initial Condition of $T_i = 300^\circ\text{k}$.	76

LIST OF FIGURES (Cont.)

<u>Figure</u>		<u>Page</u>
19	S_{uo} as a Function of Equivalence Ratio for Isooctane-Air Mixtures ($T_o = 300^\circ\text{k}$, $P_o = 1 \text{ ATM}$), R.M.S. Errors are Shown and the Curve is the Least Square Fit of Third Order Polynomial.	77
20	Contour Plot of Burning Velocity, Unburned Gas Temperature, and Normalized Unburned Density for Isooctane-Air Mixture at Equivalence Ratio of 0.8 ($P_o = 1 \text{ ATM}$, $T_o = 300^\circ\text{k}$).	78
21	Contour Plot of Burning Velocity, Unburned Gas Temperature, and Normalized Unburned Density for Stoichiometric Isooctane-Air Mixture ($P_o = 1 \text{ ATM}$, $T_o = 300^\circ\text{k}$).	79
22	Burning Velocity of Isentropes of Isooctane-Air Mixtures at Different Equivalence Ratio ϕ as a Function of Pressure with Initial Condition of $T_i = 300^\circ\text{k}$, $P_i = 1 \text{ ATM}$.	80
23	S_{uo} as a Function of Equivalence Ratio for Methanol-Air Mixtures ($T_o = 300^\circ\text{k}$, $P_o = 1 \text{ ATM}$), R.M.S. Errors are Shown, and the Curve is the Least Square Fit of 4th Order Polynomial.	81
24	Contour Plot of Burning Velocity, Unburned Gas Temperature, and Normalized Unburned Density for Methanol-Air Mixture at Equivalence Ratio of 0.8 ($P_o = 1 \text{ ATM}$, $T_o = 300^\circ\text{k}$).	82
25	Burning Velocity for Isentropes of Methanol-Air Mixtures at Different Equivalence Ratio ϕ as a Function of Pressure with Initial Condition of $T_i = 300^\circ\text{k}$ and $P_i = 1 \text{ ATM}$.	83

1.0 INTRODUCTION

The normal burning velocity S_u , of a combustible mixture is the velocity relative to the unburnt gas at which a plane flame front propagates into the mixture. It is a function of the thermodynamic properties of a combustible homogeneous gas mixture.

In the past work on spark ignition engines it has generally been assumed that the rate at which the fuel/air mixture burned was primarily controlled by the turbulent flame speed and essentially independent of the laminar flame speed. [29]* For this reason little attention has been paid to the possible effects of laminar flame speeds for practical fuels at pressure greater than one atmosphere have been made. As a result of recent analyses [27] carried out in connection with efforts to improve the efficiency and pollution characteristics of automotive engines, it now appears, however, that the laminar flame speed plays an essential role in determining several important aspects of the combustion process in spark ignition engines. Among these are:

1) The ignition delay, which in turn affects the range of equivalence ratios over which an engine can be operated and the cycle to cycle fluctuations, [27]

2) The thickness of the wall quench layers which are the primary source of unburned hydrocarbons in lean burning engines and [28]

* Numbers in brackets designate references at the end of thesis

3) The minimum ignition energy required to ignite ^[16] the charge. It also seems likely that correlations (which may not be obvious ones) exist between the laminar burning velocity and the octane rating of fuels, and the laminar burning velocity may therefore influence "knock" in engines.

Many measurements of laminar burning velocity and laminar flame speed at atmospheric conditions of temperature and pressure have been made in the past. [8,9,13,14,15,19,21,22,23,24] There have also been a few studies at elevated temperatures [12,18] or elevated pressures, [7,17,18,19,20,25,26], but very little data exist for conditions of both high temperature and pressure such as exist during combustion in an engine cylinder. [1,3,4,6,11] At the present time no reliable theory for predicting the laminar burning velocities of practical fuels exists and one can not even extrapolate the low pressure data which is available to the high pressure range of interest with any degree of confidence at all. Because of this lack of data at engine conditions it was felt to be important to develop a facility which could be used to efficiently acquire reliable laminar burning velocity data for a wide range of fuels and equivalence ratios and as a function of both temperature and pressure.

To obtain accurate data at high pressures and temperatures a spherical combustion bomb has been constructed and instrumented with ionization probes and pressure gauges. The ionization probes are used to validate the assumption of spherical symmetry necessary for our analysis. In the approach taken, the pressure record is the primary

measurement for calculating laminar burning velocities. A thermodynamic analysis of the pressure-time curve is performed, using an approximate technique to obtain burned gas properties in order to calculate the laminar burning velocities as a function of temperature and pressure. By this approach large amounts of data can be obtained from a single firing of the bomb.

Values of burning velocity for methane-air, isooctane-air, and methanol-air mixtures are obtained over a range of temperatures, pressures, and equivalence ratios. These values are fitted to some numerical relations and are compared with some results obtained by previous workers.

2.0 REVIEW OF MEASURING TECHNIQUES AND ANALYSES

Heating a fuel-air mixture up to engine temperature will start pre-flame reactions [2] and since the flame speed depends on the composition of the pre-flame gases, pre heating of the test mixture must be done on a time scale comparable to the cycle period of an engine. The most convenient way of rapidly and uniformly heating a gas is by compression and especially since high pressure is also desired for the present application, the use of some type of rapid compression system is indicated.

Burning velocity measurements have been made in conventional piston type rapid compression machines [3,4]. There is no point of direct comparison between these two studies but a burning velocity of 150-160 CM/SEC, for stoichiometric propane-air and n-heptane-air flame at 21.5 ATM and 700 °K was reported in reference 4, whereas, the authors of reference 3 claim that their results suggest a value of about 70 CM/SEC for these flames. This discrepancy is thought to be possibly due to non-quiet gas conditions existing in the rapid compression machine during the measurement of flame velocity. It has been shown that a vortex flow develops at the piston cylinder wall interface in a piston compressor [5], hence this type of device is not considered to be most suitable for achieving the required condition of temperature and pressure.

Another method of obtaining rapid compression is the use of the constant volume bomb; taking advantage of the pressure rise as combustion progresses, the burning velocity for a given mixture can be obtained over a range of temperature and pressure from a single experiment. Since flames propagate spherically from an ignition point, the ideal geometry for combustion bomb is spherical with central ignition. Quiescent gas conditions can be assured before ignition and in a spherical bomb the subsequent flow is everywhere normal to the flame front and normal to the walls. This ensures that there are no cross flames parallel to the flame front and no viscous boundary layer to destroy the flame shape, such as occur in the case of the flame propagating down a tube, right up to completion of combustion. This is important and pressure are not attained until late stages in the combustion process and the requirement to make measurements when the flame is near the vessel walls rules out other bomb geometries such as cylindrical.

Some measurements at pressure up to 70 TM and temperatures up to 650 °k, using the constant volume spherical bomb technique, have been reported [6,11]. This technique is being further developed for use in this study.

2.1 ANALYSIS OF CONSTANT VOLUME SPHERICAL BOMB COMBUSTION

2.1.1 Flow Effects

Expansion of the burnt gas behind the flame front indicates

a radial flow velocity S_g in the unburnt gas causing the flame velocity S_f to be faster than the burning velocity S_u by relation:

$$S_u = S_f - S_g \quad (1)$$

Where:

S_u is burning velocity

S_f is flame velocity

S_g is unburnt gas velocity

Figure 1 is an $r-t$ diagram showing the gas particle and flames front trajectories calculated for the case of a stoichiometric methane-air mixture initially at atmospheric conditions. The calculations were performed using the approximation of frozen combustion, constant specific heats and constant burning velocity, hence, the results are not accurate but qualitatively demonstrate several aspects of the combustion process. First it can be seen that gas particles originally near the center of the bomb have been accelerated to a high velocity by the time they are overtaken by the flame front. This is demonstrated more clearly in Figure 2 which shows the ratio of flame front velocity $S_f = S_u + S_g$, to the burning velocity as function of flame front location. The flame front velocity is initially an order of magnitude greater than the burning velocity, hence independent measurements of S_f and S_g in order to determine S_u are unlikely to yield accurate data except at large radii $\approx 80\%$ of the bomb radius. In addition, the initial pressure rise is very slow so that the

pressure record is not a sensitive monitor of the early stages of the combustion process. However, burning velocity measurements at high pressure have been made by monitoring the initial flame front velocity and determining the gas velocity from a thermodynamic calculation of the expansion ratio across the flame front. [7]

2.1.2 Burning Velocity Determination From the Pressure Record

In contrast to the direct measurement of the flame velocity S_f and unburnt gas velocity S_g , the use of pressure record to determine burning velocity requires the knowledge of thermodynamic properties of the combustible mixture and the burnt products and requires assumptions to be made about the nature of the combustion process in the bomb. However, pressure measurements have the advantage of being easy to make and of giving a continuous record, thus yielding data over a range of conditions from a single experiment. Unfortunately, the proper interpretation of the pressure record is a problem. Several closed forms of "Burning Velocity Equation" have been proposed [6,8,9] and the results obtained from a single pressure record using the various equations are compared in Figure 3 taken from reference 8. It is clear from Figure 3 that the different interpretations of the pressure record do not compare well and this must be due to the different assumptions made about the combustion process, some of which will be shown to be inaccurate.

The assumptions of thin flame and equilibrium of the burnt gas are considered to be reasonable approximations, however, the assumptions of frozen post-flame composition and of constant specific heats are not good approximations.

One of the difficulties associated with the interpretation of the pressure record is that the gradients of temperature and density develop behind the flame front which give rise to significant variations in composition and specific heat in both space and time. The presence of a density gradient when the flame contacts the vessel walls is evident from Figure 1 which shows that gas particles are not returned to their initial locations. Of more importance is the temperature gradient. The extreme of thermodynamic conditions experienced by the burnt gas occur at the center of the bomb for $t=0$ and $t=1.0$ i.e., completion of combustion. Both frozen and equilibrium specific heats for burnt gas of stoichiometric mixture of methane-air have been calculated and are shown in the table below

P	T	C_{p_f}	C_{p_e}
ATM	°k	CAL/gm°k	CAL/gm°k
1	2230	0.360	0.533
10	3480	0.373	1.240

It can be seen that equilibrium specific heat differs a lot from frozen specific heat even at low pressures and this difference increases as temperature and pressure of fuel-air mixture increases, therefore, it is clear that the approximations of frozen post-flame composition and constant specific heat are unacceptable even in the case where the initial conditions are 1 atmosphere and 300°k. For the present study the bomb can be pre-heated which would result in higher flame temperature and larger deviations from the above approximations. The mathematical problem of formulating a closed form of burning velocity equation in terms of measurable quantities such as pressure or flame radius, and accommodating the variation of specific heats is intractable. However, with the availability of fast thermodynamic equilibrium computer codes this is not a problem, and it is felt that the burning velocity equations which have been proposed in the literature should no longer be used to analyze combustion bomb data, (except for approximate studies).

3.0 EXPERIMENTAL APPARATUS

3.1 Combustion Bomb

The bomb must be large enough so that measurements can be made on flame front, the curvature of which is sufficiently small such that it approximates a plane flame front. The bomb should also be designed so that the thermal gradients, which develop behind flame front, are not capable of inducing significant heat conduction during the time of the experiment. It is, of course, also desirable to keep the size of the combustion bomb small for convenience in machining and operating of the apparatus. A 6 inch, I.D. combustion bomb was selected as a reasonable compromise between these requirements. The combustion bomb was designed to withstand a pressure of 10,000 psi with a factor of safety. The combustion bomb material is 4150FM alloy steel in the annealed condition with a 3/4 inch wall thickness. The clamp Bolts are 3/4 inch socket head cap screws with a minimum tensile strength of 56,750 lb. Windows and other fittings are of a small diameter so that the total load on them is small (< 1000 lb), and strength is not a problem. The O-ring seals are made of viton, a flourocarbon which has excellent resistance to heat, chemicals, and oil. Figure 4 shows the location and purpose of ports in the combustion bomb.

3.2 Spark Plugs and Electrodes

Standard 14-mm spark plugs with extended stainless steel

electrodes, which are tapered to a point at their tips, were used to form the spark gap at the center of the bomb. A standard coil ignition system was used for producing the spark.

3.3 Ionization Probes

The arrival time of the flame front at the wall was measured using ionization probes. There are three ionization probe positions on the perimeter of the combustion bomb, two of which are diametrically opposed. All are flush with spherical inner surface of the combustion bomb. These probes are used to check for spherical symmetry of the flame propagation. The details of the probe are given in Figure 5. The electrical circuit which was used with ionization probes is shown in Figure 6.

The associated plumbing of the experimental facilities is shown in Figure 7.

3.4 Data Collection

An oscilloscope triggered by the spark was used to record combustion bomb pressure and ionization probe signals as functions of time. An ideal oscilloscope display is shown in Figure 8, if the electrodes are exactly at the center of combustion bomb, and the mixture of air and fuel is homogeneous. It can be seen the pressure rises as a function of time up to a maximum value, at that point flame quenches at the wall and there are two ideal pressure

traces shown after the maximum pressure point, one indicates that if there is no heat transfer from burned gases to the combustion bomb wall after the flame quenches, the pressure will stay constant. The other trace shows pressure decreasing after the flame quenches at the wall because heat transfer occurs from combustion products to the wall after flame quenches. There are three ionization probe signals shown in the graph. These signals occur for ideal pressure-traces at the same time that maximum pressure occurs.

The pressure-time curve and ionization probe signal shown in Figure 9 are typical if the electrodes are not at the center of the combustion bomb or the mixture of air-fuel is not homogeneous. In this case the flame will not be symmetric with respect to the center of the combustion bomb, therefore, it hits one side of the combustion bomb wall before the other side and the pressure trace will look like the one drawn on the graph, and the ionization probe signals will not occur at the same time. Figure 10 shows an actual oscilloscope display for methane-air mixture at equivalence ratio of 0.9 and initial atmospheric condition. It can be seen that the ionization probe signals occur at the same time but about 5 MSEC ahead of peak pressure. The reason for this is not known but experiments indicate that photo emission is an important factor.

4.0 ANALYSIS OF PRESSURE - TIME DATA

The thermodynamic model of Martin and Heywood [10] was used to calculate thermodynamic properties of burned and unburned mixture at any time in the combustion process. The analysis uses conservation of mass and the first law of thermodynamics. We can write:

$$\bar{v} \equiv \frac{V}{M} = x \bar{v}_b + (1-x) \bar{v}_u \quad (2)$$

$$\bar{e} \equiv (E_o - W - Q) / M = x \bar{e}_b + (1-x) \bar{e}_u \quad (3)$$

where

V is the combustion bomb volume

M is the total charge mass, air and fuel

\bar{v} is the average specific volume of the charge

x is the mass fraction of charge that is burnt

b refers to the burnt portion of the charge

u refers to the unburnt portion of the charge

\bar{v}_b, \bar{v}_u are the appropriate average specific volumes

E_o is the total energy of the charge at some reference time t_o

$W = \int_{t_o}^t p dv = 0$ is the total work done since t_o

Q is the cumulative heat transfer since t_o which is assumed to

be negligible since heat transfer from unburned mixture (300 °k - 500 °k) occurs for a very short period of time (about 50 MSEC) to the combustion bomb wall at 300

\bar{e} , \bar{e}_b , \bar{e}_u are the appropriate average specific internal energies

Assuming that at any time the flame remains smooth and spherical with no convective rise of the burnt gases; there are no pressure gradients within the rigid vessel, the unburnt gas is compressed during the explosion isentropically with variable specific heat ratio, therefore, the thermodynamic properties of unburned mixture (T_u , \bar{v}_u , \bar{e}_u) can be calculated for given pressure, and equivalence ratio. The burnt part of the charge can be approximated as homogeneous, at equivalence ratio ϕ_0 and temperature \bar{T}_b , and pressure P, where \bar{T}_b and P change with time. With these assumptions, we can write

$$\bar{v}_b = v_b (P, \bar{T}_b) \quad (4)$$

$$\bar{e}_b = e_b (P, \bar{T}_b) \quad (5)$$

The values of \bar{v}_b and \bar{e}_b are known for given P, \bar{T}_b , and ϕ_0 using the Martin and Heywood model [10].

Equations (2) and (3) were solved for two the unknowns \bar{T}_b and X using Newton-Raphson iteration method. For this technique we rewrite equations (2) and (3) as follows:

$$F_1 = \bar{e} - (1-X) \bar{e}_u - X \bar{e}_b \quad (6)$$

$$F_2 = \bar{v} - (1-X) \bar{v}_u - X \bar{v}_b \quad (7)$$

The elements of the Jacobian matrix are defined as

$$A_{11} = -X \frac{\partial \bar{e}_b}{\partial \bar{T}_b} = -X (c_p + P \left(\frac{\partial \bar{\rho}_b}{\partial T} \right)_P / \bar{\rho}_b^{-2}) \quad (8)$$

$$A_{12} = \bar{e}_u - \bar{e}_b \quad (9)$$

$$A_{21} = -X \frac{\partial \bar{v}_b}{\partial \bar{T}_b} = X \left(\frac{\partial \bar{\rho}_b}{\partial T} \right)_P / \bar{\rho}_b^{-2} \quad (10)$$

$$A_{22} = \bar{v}_u - \bar{v}_b \quad (11)$$

Where:

c_p is the partial derivative of enthalpy with respect to temperature at constant pressure and equivalence ratio

$\bar{\rho}_b$ is the average density of burned gas

To start the iteration guesses are made for \bar{T}_b and X (usually based on the last time step) and the following equation is solved

$$\begin{bmatrix} A_{11} & A_{12} \\ A_{21} & A_{22} \end{bmatrix} \begin{bmatrix} \delta_1 \\ \delta_2 \end{bmatrix} = \begin{bmatrix} -F_1 \\ -F_2 \end{bmatrix} \quad (12)$$

The K+1 estimates are defined from the Kth estimate

$$\bar{T}_{b_{K+1}} = \bar{T}_{b_K} + \delta_1 \quad (13)$$

$$X_{K+1} = X_K + \delta_2 \quad (14)$$

The following definitions result from the assumptions of spherical symmetry and mass conservation

$$V_b = X \bar{v}_b \quad M = \frac{4}{3} \pi R_f^3 \quad (15)$$

$$R_f = (3X \bar{v}_b M / 4\pi)^{1/3} \quad (16)$$

$$A_f = 4 \pi R_f^2 \quad (17)$$

$$S_u = M \dot{X}(t) / \bar{\rho}_u A_f \quad (18)$$

where

R_f is the radius of flame

A_f is area of flame

S_u is laminar burning velocity

\dot{X} is rate of mass fraction burned which was obtained by taking the derivative of X with respect to time numerically

Typical results are shown in Figure 11. The broken lines are the calculated burning velocities for methane-air mixture at three different equivalence ratios of 0.8, 1.0, and 1.2 with different initial pressures of 1, 2.04, 4.08, and 8.16 ATM with initial temperature of 300°k. The point "P" indicates the point of discontinuity of ionization probes. The smooth curves are the fitted burning velocity curves which will be discussed later, and the dashed-curves are extrapolation of the fitted curves. Figure 12 shows the calculated burning velocity for isooctane-air mixtures at initial conditions of 1 ATM pressure and temperature of 300°k with equivalence ratio ranging from 0.7 to 1.6. Figure 13 represents the calculated burning velocity for methanol-air mixtures at initial conditions of 1 ATM pressure and temperature of 300°k with equivalence ratio ranging from 0.7 to 1.5

5.0 DISCUSSION OF RESULTS

5.1 Parametric Fit of Measured Burning Velocities

The calculated burning velocities for methane, isooctane, and methanol at different unburned mixture densities and temperatures have been fitted to the following relation

$$S_u = S_{u0} \left(\frac{T_u}{T_{u0}} \right)^\alpha \left(\frac{\rho_u}{\rho_{u0}} \right)^\beta \quad (19)$$

where

S_u is laminar burning velocity in CM/SEC

S_{u0} is laminar burning velocity at reference point

T_u is temperature of unburned mixture in °k

T_{u0} is reference temperature = 300°k

ρ_u is density of unburned mixture in GM/CC can be calculated using equations 22, 23, and 24 for given pressure, temperature, and equivalence ratio of unburned mixture.

ρ_{u0} is density of unburned mixture at 300°k and 1 atm pressure in GM/CC can be evaluated using equations 22,23, and 24.

α, β are fitted exponents.

There is also another parameter of interest which is defined as

$$\epsilon = \left(\frac{\partial \ln S}{\partial \ln \rho_u} \right)_{u \text{ const.}} = \alpha \left(\frac{\partial \ln T}{\partial \ln \rho_u} \right)_{u \text{ const.}} + \beta \quad (20)$$

entropy entropy

and using isentropic relations between density and temperature we get

$$\epsilon = \alpha (\gamma_u - 1) + \beta \quad (20-a)$$

where

γ_u is specific ratio of unburned mixture

Using isentropic relation $\frac{T}{T_o} = \left(\frac{\rho}{\rho_o} \right)^{\gamma_u - 1}$ in equation (19) gives the following relation

$$S_u = S_{uo} \left(\frac{\rho_u}{\rho_o} \right)^{\alpha(\gamma_u - 1)} \left(\frac{\rho_u}{\rho_{uo}} \right)^{\beta} = S_{uo} \left(\frac{\rho_u}{\rho_{uo}} \right)^{\alpha(\gamma_u - 1) + \beta} \quad (20-b)$$

substituting equation (20-a) in (20-b) would result

$$S_u = S_{uo} \left(\frac{\rho_u}{\rho_{uo}} \right)^{\epsilon} \quad (21)$$

Therefore burning velocity for isentropes can be determined by

knowing the parameter ϵ , but it should be noticed that equations (20) through (21) apply only to the cases where initial temperature and pressure is the same as reference condition.

The parameters S_{u0} , α , β , and ϵ have been determined using least-square method. The mathematics involved is described in Appendix 1.

The density of unburned mixture at given pressure, temperature, and equivalence ratio can be calculated by using the following equations:

Methane-air mixture:

$$\rho = \frac{.012187 P}{T} \left(\frac{137.28 + 8\phi}{4.76 + .5\phi} \right) \quad (22)$$

Isooctane-air mixture

$$\rho = \frac{.012187 P}{T} \left(\frac{137.28 + 9.12 \phi}{4.76 + 0.08 \phi} \right) \quad (23)$$

Methanol-air mixture

$$\rho = \frac{.012187 P}{T} \left(\frac{137.28 + 21.33 \phi}{4.76 + 0.667 \phi} \right) \quad (24)$$

where:

ρ is density of mixture in GM/CC

p is pressure of mixture in ATM

T is temperature of mixture in degree K

ϕ is equivalence ratio of mixture

5.2 Methane-Air Mixture

The laminar burning velocities for methane-air mixture at different equivalence ratio and pressure were calculated and results were fitted to equation (19). Methane-air mixtures were burned at four different initial pressure of 1, 2.04, 4.08, and 8.16 ATM at equivalence ratios of 0.8, 1.0 and 1.2. In these experiments initial temperature for all cases was 300°k. Table 1 shows the parameters S_{uo} , α, β, ϵ , and their r.m.s. fluctuations for methane-air mixture

Table 1

Parameters	S_{uo} , α , β , ϵ and their r.m.s. fluctuations for methane-air mixture			
ϕ	$S_{uo} + \Delta S_{uo}$ (CM/SEC)	$\alpha \pm \Delta\alpha$	$\beta \pm \Delta\beta$	$\epsilon \pm \Delta\epsilon$
0.8	29.5±0.94	1.53±0.09	-0.38±0.01	0.17±0.01
1.0	35.86±0.77	1.29±0.06	-0.26±0.01	0.19±0.01
1.2	31.32±1.09	1.52±0.09	-0.38±0.01	0.19±0.02

Figure 14 shows laminar burning velocity of methane-air mixture at reference condition ($P_o = 1 \text{ ATM}$, $T_o = 300^\circ\text{k}$) and their r.m.s. fluctuations as a function of equivalence ratio. The curve is the best fit of polynomial of degree 4 using least-square method weighted by the r.m.s. fluctuations. The equations for this curve turned out to be

$$S_{uo} = 11.64 - 34.92 \phi + 74.88 \phi^2 + 40.79 \phi^3 - 56.2 \phi^4 \quad (25)$$

The calculated and fitted burning velocity of methane-air mixture at equivalence ratio of 0.8, 1.0, and 1.2 with different initial pressures are shown in Figure 11. The broken lines represent the experimental values of burning velocity, and the smooth curves show the fitted burning velocity using equation (19), and dashed-lines are extrapolation of the fitted curve. It can be seen that the burning velocity is at highest at stoichiometric mixture, and burning velocity in rich region is slightly more than lean mixtures. Figure 15 shows a contour plot of unburned temperature, normalized unburned density (ρ_u/ρ_o), and laminar burning velocity for methane-air mixture at equivalence ratio of 0.8. The reference point is $P_o = 1 \text{ ATM}$, $T_o = 300^\circ\text{k}$. The smooth curves are constant burning velocity curves, and the dashed lines are isentropes representing locus of experimental measurements. Using this figure burning velocity can be calculated up to 50 ATM pressure and 550 °k unburned temperature. Burning

velocity can be read from Figure 15 by aid of the following

relation:

$$\frac{\rho_u}{\rho_o} = \left(\frac{P}{P_o}\right) \left(\frac{T_o}{T_u}\right) \quad (26)$$

Figures 16 and 17 represent the relations between normalized unburned density, unburned temperature, and burning velocity for methane-air mixtures at equivalence ratios of 1.0 and 1.2. Burning velocity at any pressure and temperature can be read from graphs by using equation (26).

Burning velocities of methane-air mixture at initial condition of 1 ATM pressure and 300 °k temperature with equivalence ratio varying from 0.8 to 1.3 were calculated, the results are plotted in Figure 18. It can be seen that burning velocity is highest at equivalence ratio of 1.05. The dashed lines are extrapolation of burning velocities.

5.3 Comparison of Values of Burning Velocity For Methane-Air Mixture

There are many different equations for burning velocity of methane-air mixture reported in literature.

Bradley and Micheson [1] used the following relationship for stoichiometric methane-air mixture:

$$S_u = (10 + 0.000371T^2) - 0.0052T^{1.5} \log p \quad (27)$$

in which T is °k and P in atmospheres. This equation differs about 10% with calculated burning velocity using equation (19) and

Table 1 for the isentropic compression from 300 °k and one atmosphere. Equation (27) shows decreasing in burning velocity for isentrope having initial temperature of 300°k and 4 ATM pressure which indicates that equation (27) is not dependable for high initial pressure condition.

Babkin and Kozachenko [11] used the following relation for stoichiometric methane-air mixture in the range of 323 - 473 °k and 1-23 ATM:

$$S_u = \left(\frac{T}{100}\right)^2 (3.18 - 1.53 \log P) \quad (28)$$

This relation predicts lower burning velocity than calculated burning velocity using equation (19) and Table 1 up to temperature of 350 °k and it is in very good agreement with equation (19) and Table 1 in higher range of temperature.

5.4 Isooctane-Air Mixture

Burning velocity for isooctane-air mixture at different equivalence ratio and pressure was calculated and results were fitted to equation (19). Since isooctane vapor pressure at room temperature is about 45 mm Hg it was not possible to make isooctane-air mixture with initial pressure of more than 3.06 ATM at room temperature, therefore, isooctane-air mixtures were burned at three different initial pressures of 1, 2.04, and 3.06 ATM at equivalence ratios of 0.8, 1.0. and 1.2. In these experiments initial tempera-

ture for all cases was 300°k. Table II shows the calculated values of S_{uo} , α , β , ϵ , and their r.m.s. fluctuations for isooctane-air mixture.

Table II

Parameters S_{uo} , α, β, ϵ , and their r.m.s. fluctuations for isooctane-air mixture

ϕ	$S_{uo} \pm \Delta S_{uo}$ (CM/SEC)	$\alpha \pm \Delta \alpha$	$\beta \pm \Delta \beta$	$\epsilon \pm \Delta \epsilon$
0.8	33.43±1.52	2.41±0.15	-0.36±0.03	0.42±0.02
1.0	35.25±1.33	1.85±0.13	-0.12±0.02	0.45±0.01
1.2	27.63±1.04	1.30±0.14	0.05±0.03	0.46±0.01

Figure 19 shows laminar burning velocity of isooctane-air mixture at reference condition ($P_o=1$ ATM, $T_o=300^\circ k$) as a function of equivalence ratio. The r.m.s. fluctuations are shown on the graph and the smooth curve is the best fit of polynomial of degree 4 using least-square method weighted by the r.m.s. fluctuations. The equation for this curve is:

$$S_{uo} = - 20.69 + 98.66 \phi + 26.63 \phi^2 - 11.34 \phi^3 + 39.95 \phi^4 \quad (29)$$

A contour plot of normalized unburned density, unburned temperature, and burning velocity for isooctane-air mixture at equivalence ratio of 0.8 is plotted in Figure 20. The same kind

of plot for isooctane-air mixture at equivalence ratio of 1.0 is plotted in Figure 21. In these graphs the smooth curves represent constant burning velocity and the dashed lines are isentropes representing locus of experimental measurements.

Burning velocity can be read by using these charts and equation (26) at given pressure, temperature, and equivalence ratio by considering that $T_o = 300$ °k and $P_o = 1$ ATM = 14.7 psia. The maximum experimental pressure and temperature were 20 ATM and 500 °k but the results on these graphs are extrapolated to the pressure of 25 ATM and up to 550 °k temperature. It can be noticed that at constant pressure, burning velocity of isooctane-air mixture is less than burning velocity of methane-air mixture at low temperature and S_u for isooctane-air mixture exceeds burning velocity of methane-air mixture as unburned temperature increases.

Isooctane-air mixtures were burned at initial pressure of 1 ATM and temperature of 300 °k with the range of equivalence ratio from 0.7 to 1.6, and the results are plotted in Figure 12. The broken lines are the experimental points and the smooth curves are fitted burning velocity using equation (19), and the dashed lines are the extrapolation of the fitted curves. This figure shows that burning velocity of isooctane-air mixture at lean side is slightly more than the rich mixtures. Figure 22 represents burning velocity of isooctane-air mixture at different equivalence ratio, the maximum burning velocity occurs at stoichiometric mixture, and the

minimum is at equivalence ratio of 1.6.

5.5 Comparison of Values of Burning Velocity for Isooctane-Air Mixture

Different authors have proposed different equations and values for burning velocity of isooctane-air mixtures, Babkin and Kozachenko [6] found the following relation for stoichiometric isooctane- air mixture:

$$S_u = (404 \log T - 1008) P^{-0.39 + 0.40(T/1000)} \quad (30)$$

Where T and P are in °k and ATM.

Equation (30) predicts burning velocity of 22 CM/SEC for the mixture of 5 ATM pressure and temperature of 375 °k which is very low prediction while Heimel and Weast [12] declare of burning velocity of 47 CM/SEC for the same condition. Equation (19) by aid of Table II predicts burning velocity of 45 CM/SEC which is more reasonable by considering the assumptions involved in deriving equation (30) and the one used by authors of reference [12].

5.6 Methanol-Air Mixture

Burning velocity for methanol-air mixtures at different equivalence ratio and pressure was calculated and results were fitted to equation (19). Vapor pressure of methanol at room temperature is 100 mm Hg, therefore, the maximum initial pressure of methanol-air mixture was 2.04 ATM which occurred at equivalence ratio of 0.8. Methanol-air mixtures at equivalence ratio of 0.8

were burned at different initial pressure 1 and 2.04 ATM with initial temperature of 300°k. Table III represents the calculated values of S_{uo} , α , β , ϵ , and their r.m.s. fluctuations for different equivalence ratios of methanol-air mixtures to be used in equation (19).

Table III

Parameters S_{uo} , α, β, ϵ , and their r.m.s. fluctuations for methanol-air mixture

ϕ	$S_{uo} \pm \Delta S_{uo}$ (CM/SEC)	$\alpha \pm \Delta \alpha$	$\beta \pm \Delta \beta$	$\epsilon \pm \Delta \epsilon$
0.8	31.72±2.09	2.12±0.30	-0.28±0.07	0.45±0.02
1.0	44.33±1.48	16.30±7.55	6.05±2.60	0.50±0.01
1.2	40.80±1.14	13.56±5.18	-4.13±1.77	0.47±0.01

Figure 23 shows laminar burning velocity of methanol-air mixture at reference condition ($P_o=1$ ATM, $T_o=300$ °k) as a function of equivalence ratio. The r.m.s. fluctuations are shown on the graph and the smooth curve is the best fit of polynomial of third degree using least-square method weighted by the r.m.s. fluctuations. The equation of this curve turned out to be

$$S_{uo} = 299.22 + 647.87 \phi - 485.67 \phi^2 + 110.75 \phi^3 \quad (31)$$

A contour plot of unburned temperature, normalized unburned density, and burning velocity for methanol-air mixture at equivalence ratio of 0.8 is shown in Figure 24. The smooth curves are constant burning velocity and dashed lines are isentropes representing locus of experimental measurements. The reference condition is at $P_o = 1 \text{ ATM}$ $T_o = 300 \text{ }^\circ\text{k}$. Burning velocity at each pressure and temperature can be read by using equation (26). This chart covers the temperature range up to 550 $^\circ\text{k}$ and pressure range of up to 15 ATM. By comparing Figure 15 which is burning velocity of methane at $\phi = 0.8$, and Figure 21 which is burning velocity of isooctane at $\phi = 0.8$, and Figure 24 it can be seen that at constant equivalence ratio and same pressure and temperature burning velocity of methanol-air mixture is higher than burning velocity of methane-air mixture and isooctane-air mixture.

Methanol-air mixtures with initial condition of 1 ATM pressure and 300 $^\circ\text{k}$, and different equivalence ratio ranging from 0.7 to 1.5 were burned, and calculated burning velocity for these cases are represented in Figure 13. The broken lines show the calculated burning velocity and the smooth curves are the fitted burning velocity using equation (19). This Figure shows that burning velocity peaks at stoichiometric methanol-air mixture and decreases in both rich and lean mixtures,

Figure 25 shows burning velocity of methanol-air mixtures at different equivalence ratios.

5.7 Comparison of Values of Burning Velocity For Methanol-Air Mixture

There are not many calculated burning velocity of methanol-air mixture in literature Gibbs and Calcote^[13] have reported burning velocity of 34.5 CM/SEC for methanol-air mixture at equivalence ratio of 0.8 and initial condition of 1 ATM pressure and room temperature while equation (19) and Table III suggest a value of 31.72 CM/SEC for the Same conditions.

6.0 CONCLUSIONS AND SUGGESTIONS

A laminar burning velocity measurement facility has been constructed and the data analysis technique verified. A survey has been carried out of experimental values of burning velocity of methane-air, isooctane-air, and methanol-air mixtures. This reveals a wide scatter, dependent to some extent on experimental method. A thermodynamic analysis is used to calculate laminar burning velocities once a pressure-time trace of the combustion process is obtained. An equilibrium program is used to assure that the specific heats of the burned gases are obtained correctly. Ionization probes are used to assure that spherical symmetry exists. The advantage of the data analysis technique used is the multitude of data that can be obtained from a single pressure-time trace. Laminar burning velocities for methane-air, isooctane-air, and methanol-air mixtures with initial condition of 300 °k temperature, 1-8 Atmosphere pressure, and equivalence ratio of 0.7 - 1.6 have been calculated. Results are presented graphically and numerically.

The suggestions for future work will be:

(a) Using heat transfer gauges instead of ionization probes because it can be seen from Figure 10 that ionization probe signals occur a short time ahead of the time which flame quenches. Even though these probes represent the spherical symmetry of the flame but their discontinuity before quenching time is mysterious,

therefore, it will be better to design and build heat transfer gauge to show the position of the flame front.

(b) To use an electrical differentiator to get rid of the fluctuation in laminar burning velocity which are the results of numerical calculations.

(c) To raise the temperature of combustion bomb and fuel before igniting the combustible mixture. The reason is to increase the initial temperature of fuel-air mixture in order to vaporize the liquid fuels and make the same condition for fuel-air mixtures as they have in combustion engines.

APPENDIX I BURNING VELOCITY FIT AND ERROR ANALYSIS

The calculated burning velocities at constant equivalence ratio were fitted to the following equation:

$$S_u = S_{uo} \left(\frac{T_u}{T_{uo}} \right)^\alpha \left(\frac{\rho_u}{\rho_{uo}} \right)^\beta \quad (32)$$

It follows that the error would be

$$\overline{\delta S^2} = \frac{1}{N} \sum_{i=1}^N \left[S_{ui} - S_{uo} \left(\frac{T_{ui}}{T_{uo}} \right)^\alpha \left(\frac{\rho_{ui}}{\rho_{uo}} \right)^\beta \right]^2 \quad (33)$$

Where:

N is the number of data points.

In order to make this simple we introduce new notations

$$\tilde{T}_i = \frac{T_{ui}}{T_{uo}} \quad (34)$$

$$\tilde{\rho}_i = \frac{\rho_{ui}}{\rho_{uo}} \quad (35)$$

Therefore:

$$\overline{\delta S^2} = \frac{1}{N} \sum_{i=1}^N S_{ui}^2 \left(1 - \frac{S_{uo}}{S_{ui}} \tilde{T}_i^\alpha \tilde{\rho}_i^\beta \right)^2 \quad (36)$$

The expression in parenthesis can be written in logarithm form if its value is close to zero. Then,

$$\overline{\delta S^2} = \frac{1}{N} \sum_{i=1}^N S_{ui}^2 \left(\ln \left(\frac{S_{ui}}{S_{uo} \tilde{T}_i^{\alpha} \tilde{\rho}_i^{\beta}} \right) \right)^2 \quad (37)$$

$$\overline{\delta S^2} = \frac{1}{N} \sum_{i=1}^N S_{ui}^2 (\ln S_{ui} - \ln S_{uo} - \alpha \ln \tilde{T}_i - \beta \ln \tilde{\rho}_i)^2 \quad (38)$$

In order to calculate S_{uo} , α , and β we differentiate the above expression with respect to $\ln S_{uo}$, α , and β and set the results equal to zero. This would give the following 3 equations:

$$0 = \sum_{i=1}^N S_{ui}^2 (\ln S_{ui} - \ln S_{uo} - \alpha \ln \tilde{T}_i - \beta \ln \tilde{\rho}_i) \quad (39)$$

$$0 = \sum_{i=1}^N S_{ui}^2 (\ln S_{ui} - \ln S_{uo} - \alpha \ln \tilde{T}_i - \beta \ln \tilde{\rho}_i) \ln \tilde{T}_i \quad (40)$$

$$0 = \sum_{i=1}^N S_{ui}^2 (\ln S_{ui} - \ln S_{uo} - \alpha \ln \tilde{T}_i - \beta \ln \tilde{\rho}_i) \ln \tilde{\rho}_i \quad (41)$$

Using the following notation:

$$W_i = S_{ui}^2 \quad (42)$$

$$X_i = \ln \tilde{T}_i \quad (43)$$

$$Y_i = \ln \tilde{\rho}_i \quad (44)$$

$$Z_i = \ln S_{ui} \quad (45)$$

$$\text{Vector } [a] = \begin{bmatrix} \ln A \\ \alpha \\ \beta \end{bmatrix} \quad (46)$$

Rearranging set of equation (39), (40), (41) and introducing coefficient matrix \bar{A} as:

$$\bar{A} = \begin{bmatrix} \sum_{i=1}^N W_i & \sum_{i=1}^N W_i X_i & \sum_{i=1}^N W_i Y_i \\ \sum_{i=1}^N W_i X_i & \sum_{i=1}^N W_i X_i^2 & \sum_{i=1}^N W_i X_i Y_i \\ \sum_{i=1}^N W_i Y_i & \sum_{i=1}^N W_i X_i Y_i & \sum_{i=1}^N W_i Y_i^2 \end{bmatrix} \quad (47)$$

and introducing vector \bar{b} as

$$\bar{b}^T = \left[\begin{array}{ccc} \sum_{i=1}^N W_i Z_i & \sum_{i=1}^N W_i Z_i X_i & \sum_{i=1}^N W_i Y_i Z_i \end{array} \right] \quad (48)$$

it would result:

$$\bar{a} \bar{A} = \bar{b} \quad (49)$$

$$\bar{a} = \bar{A}^{-1} \bar{b} \quad (50)$$

Inverse matrix \bar{A}^{-1} was determined using Gauss-Jordan elimination method.

Therefore:

$$a_i = \sum_{J=1}^3 A_{iJ}^{-1} b_J \quad i=1,2,3 \quad (51)$$

To calculate the deviation in a's it follows:

$$\delta a_i = \sum_{J=1}^3 A_{iJ}^{-1} \left(\sum_{k=1}^N \frac{\partial b_J}{\partial S_{uk}} \delta S_{uk} \right) \quad (52)$$

$$\delta a_i = \sum_{k=1}^N \delta S_{uk} \left(\sum_{J=1}^3 A_{iJ}^{-1} \frac{\partial b_J}{\partial S_{uk}} \right) \quad (53)$$

$$\overline{\delta a_i^2} = \sum_{k=1}^N \overline{\delta S_{uk}^2} \left(\sum_{J=1}^3 A_{iJ}^{-1} \frac{\partial b_J}{\partial S_{uk}} \right)^2 \quad (54)$$

$$\overline{\delta a_i^2} = \overline{\delta S^2} \sum_{k=1}^N \left(\sum_J A_{iJ}^{-1} \frac{\partial b_J}{\partial Z_k} \frac{dZ_k}{dS_{uk}} \right)^2 \quad (55)$$

$$\overline{\delta a_i^2} = \overline{\delta S^2} \sum_{k=1}^N \left(A_{i1}^{-1} + A_{i2}^{-1} X_k + A_{i3}^{-1} Y_k \right)^2 W_k \quad (56)$$

Three parameters and their r.m.s. fluctuations were calculated by solving equations (51) and (56). There is another parameter of interest namely ϵ which was introduced in Chapter 5 and is defined as:

$$\epsilon = \left(\frac{\partial \ln S_u}{\partial \ln \rho_u} \right)_{\text{const. entropy}} = \alpha(\gamma_u - 1) + \beta \quad (20)$$

Solving equation (20) for β and substituting in equation (32) would result

$$S_u = S_{u0} T^{\frac{\alpha}{\rho}} \epsilon^{-\alpha(\gamma_u - 1)} \quad (57)$$

Where γ_u is specific heat ratio of unburned mixture and was determined for different equivalence ratio of fuel-air mixtures.

The procedure of equations (32) to (56) was done for equation (57) and parameters S_{u0} , α , ϵ , and their r.m.s. deviations were calculated. Table IV shows parameters S_{u0} , α , β , ϵ , and their deviations for methane-air mixture as a function of equivalence ratio. It can be noticed that for mixtures of equivalence ratio of 0.8, 1.0, and 1.2 the error in calculations α is very small while for the other cases the error is much bigger, the reason is there were four sets of data with different initial pressure for mixtures of having equivalence ratio of 0.8, 1.0, and 1.2 while for the other cases there was only one set of data having initial pressure of 1 ATM. Meanwhile $\Delta\epsilon$ is a small number for cases where $\Delta\alpha$ and $\Delta\beta$ are large which represents that the deviation of linear combination of α and β for isentrope is small.

Table V and VI represents the parameters S_{u0} , α , β , ϵ , and their r.m.s. fluctuations for isooctane-air and methanol-air mixtures as

a function of equivalence ratio. The same characteristics for α , β , and ϵ can be noticed as was shown for methane-air mixtures.

APPENDIX II ANALOG DIFFERENTIATOR AND CORRESPONDING ANALYSIS

It is desired to build an analog differentiator in order to get the time derivative of pressure trace. A differentiator has already been designed and built, but its time constant is a function of frequency which is not great, therefore, the work is continuing to build a suitable analog differentiator. In order to continue the analysis first the time derivative of pressure (\dot{p}) should be integrated numerically, then the analysis of section 4 should be used to determine mass fraction burned x , and thermodynamic properties of burned and unburned gas at any time. In order to get time derivative of mass fraction burned \dot{X} we start by taking derivatives of equations (2) and (3):

$$\dot{\bar{v}} = \dot{X} (\bar{v}_b - \bar{v}_u) + X \dot{\bar{v}}_b + (1-X) \dot{\bar{v}}_u = 0 \quad (58)$$

$$\dot{\bar{e}} = \dot{X} (\bar{e}_b - \bar{e}_u) + X \dot{\bar{e}}_b + (1-X) \dot{\bar{e}}_u = 0 \quad (59)$$

and knowing that:

$$\bar{e}_u = e_u(\bar{T}_u, p) \quad (60)$$

$$\bar{e}_b = e_b(\bar{T}_b, p) \quad (61)$$

$$\bar{T}_u = \bar{T}_u(p) \quad (62)$$

$$\bar{v}_u = v_u(\bar{T}_u, p) \quad (63)$$

$$\bar{v}_b = v_b(\bar{T}_b, p) \quad (64)$$

It follows that

$$\dot{\bar{e}}_u = \left(\frac{\partial \bar{e}_u}{\partial \bar{T}_u}\right)_P \dot{\bar{T}}_u + \left(\frac{\partial \bar{e}_u}{\partial P}\right)_T \dot{P} \quad (65)$$

$$\dot{\bar{e}}_b = \left(\frac{\partial \bar{e}_b}{\partial \bar{T}_b}\right)_P \dot{\bar{T}}_b + \left(\frac{\partial \bar{e}_b}{\partial P}\right)_T \dot{P} \quad (66)$$

$$\dot{\bar{T}}_u = \frac{\partial \bar{T}_u}{\partial P} \dot{P} \quad (67)$$

$$\dot{\bar{v}}_u = \left(\frac{\partial \bar{v}_u}{\partial \bar{T}_u}\right)_P \dot{\bar{T}}_u + \left(\frac{\partial \bar{v}_u}{\partial P}\right)_T \dot{P} \quad (68)$$

$$\dot{\bar{v}}_b = \left(\frac{\partial \bar{v}_b}{\partial \bar{T}_b}\right)_P \dot{\bar{T}}_b + \left(\frac{\partial \bar{v}_b}{\partial P}\right)_T \dot{P} \quad (69)$$

To calculate $\frac{\partial \bar{T}_u}{\partial P}$ we know

$$S = S(P, T) \quad (70)$$

$$dS = \left(\frac{\partial S}{\partial T}\right)_P dT + \left(\frac{\partial S}{\partial P}\right)_T dP \quad (71)$$

$$c_P = T \left(\frac{\partial S}{\partial T}\right)_P \quad (72)$$

$$\left(\frac{\partial S}{\partial P}\right)_T = - \left(\frac{\partial v}{\partial T}\right)_P \quad (\text{one of the Maxwell's Relation}) \quad (73)$$

$$dS = \frac{C_p}{T} dT - \left(\frac{\partial v}{\partial T}\right)_P dP \quad (74)$$

Since the unburned gas compresses isentropically equation (71) reduces to

$$\left(\frac{\partial \bar{T}_u}{\partial P}\right) = \left(\frac{\partial \bar{v}_u}{\partial \bar{T}_u}\right)_P \frac{\bar{T}_u}{C_{P_u}} \quad (75)$$

The quantities $\left(\frac{\partial \bar{e}_u}{\partial \bar{T}_u}\right)_P$, $\left(\frac{\partial \bar{e}_u}{\partial P}\right)_T$, $\left(\frac{\partial \bar{e}_b}{\partial \bar{T}_b}\right)_P$, $\left(\frac{\partial \bar{v}_u}{\partial \bar{T}_u}\right)_P$,

$\left(\frac{\partial \bar{v}_u}{\partial P}\right)_T$, $\left(\frac{\partial \bar{v}_b}{\partial \bar{T}_b}\right)_P$, $\left(\frac{\partial \bar{v}_b}{\partial P}\right)_T$, \bar{T}_u , and C_{P_u} can be calculated using

Martin and Heywood model [10], therefore there are two unknowns \dot{X} and $\dot{\bar{T}}$ in equations (58) and (59) to be solved for. Substituting equation (69) into equation (58).

$$\dot{X} (\bar{v}_b - \bar{v}_v) + X \left[\left(\frac{\partial \bar{v}_b}{\partial \bar{T}_b}\right)_P \dot{\bar{T}}_b + \left(\frac{\partial \bar{v}_b}{\partial P}\right)_T \dot{P} \right] + (1-X) \dot{\bar{v}}_u = 0 \quad (76)$$

rearranging the above formula

$$\dot{\bar{T}}_b = \frac{\dot{X} (\bar{v}_u - \bar{v}_b) - (1-X) \dot{\bar{v}}_u - X \left(\frac{\partial \bar{v}_b}{\partial P} \right)_T \dot{P}}{X \left(\frac{\partial \bar{v}_b}{\partial T_b} \right)_P} \quad (77)$$

Substituting equation (66) into equation (59)

$$\dot{X} (\bar{e}_b - \bar{e}_u) + X \left[\left(\frac{\partial \bar{e}_b}{\partial \bar{T}_b} \right)_P \dot{\bar{T}}_b + \left(\frac{\partial \bar{e}_b}{\partial P} \right)_T \dot{P} \right] + (1-X) \dot{\bar{e}}_u = 0 \quad (78)$$

Substituting equation (77) in (78)

$$\begin{aligned} \dot{X} (\bar{e}_b - \bar{e}_u) + \left(\frac{\partial \bar{e}_b}{\partial \bar{T}_b} \right)_P \left[\dot{X} (\bar{v}_u - \bar{v}_b) - (1-X) \dot{\bar{v}}_u - X \left(\frac{\partial \bar{v}_b}{\partial P} \right)_T \dot{P} \right] \frac{1}{\left(\frac{\partial \bar{v}_b}{\partial T_b} \right)_P} \\ + X \left(\frac{\partial \bar{e}_b}{\partial P} \right)_T \dot{P} + (1-X) \dot{\bar{e}}_u = 0 \end{aligned} \quad (79)$$

Rearranging equation (79) and solving for \dot{X} :

$$\dot{X} = \frac{[(1-X)\dot{\bar{v}}_u + X\left(\frac{\partial \bar{v}_b}{\partial P_T}\right) \dot{P}] \left(\frac{\partial \bar{e}_b}{\partial \bar{T}_b}\right) / \left(\frac{\partial \bar{v}_b}{\partial \bar{T}_b}\right) - X\left(\frac{\partial \bar{e}_b}{\partial P_T}\right) \dot{P} - (1-X)\dot{\bar{e}}_u}{(\bar{e}_b - \bar{e}_u) + (\bar{v}_u - \bar{v}_b) \left(\frac{\partial \bar{e}_b}{\partial \bar{T}_b}\right) / \left(\frac{\partial \bar{v}_b}{\partial \bar{T}_b}\right)} \quad (80)$$

Knowing rate of mass fraction burned \dot{X} , equations (15) through (18) can be used to calculate burning velocities of different fuels.

REFERENCES

1. Bradley, D. and Mitcheson, A., "Mathematical Solution for Explosion in Spherical Vessels," *Combustion and Flame* 26, 201-217 (1976).
2. Pahnke, A.J., Cohen, P.M., and Sturgis, B.M., "PREFLAME OXIDATION OF HYDROCARBONS IN A MOTORED ENGINE," *Industrial and Engineering Chemistry*, Vol. 46, No. 5, p. 1024, May 1954.
3. Halstead, M.P., Pye, D.B., and Quinn, C.P., "Laminar Burning Velocities and Weak Flammability Limits Under Engine-Like Conditions," *Combustion and Flame* 22, p. 89, 1974.
4. De Soete, G., and Brasselet, J., *Rev. Inst. Fr. Petrole*, 24, p. 1507 (1969).
5. Tabaczynski, R. J., Houtt, D.P., and Keck, J.C., "High Reynolds Number Flow in a Moving Corner," *J. Fluid Mechanics*, Vol. 42 (June 1970) p. 249.
6. Babkin, V.S., V'yun, A.V., and Kozachenko, L.S., "Determination of Burning Velocity from the Pressure Record in a Constant Volume Vessel," *Combustion, Explosion, and Shock Waves*, Vol. 3, No. 3, pp. 362-370, 1967.
7. Babkin, et al, "Effect of Pressure on Normal Flame Velocity Investigated by the Initial Section Method in a Constant Volume Vessel," *Combustion, Explosion and Shock Waves*, Vo. 2, No. 2, p. 32, 1966.
8. Rallis, C.J., and Tremeer, G.E.B., "Equations for the Determination of Burning Velocity in a Spherical Constant Volume Vessel," *Combustion and Flame* 7, No. 1, p. 51, 1963.
9. Babkin, V.S., and Kononenko, Yu.G., "Analysis of Equations for Determining the Normal Burning Velocity by the Constant Volume Bomb Technique," *Combustion, Explosion and Shock Waves*, Vol. 5, No. 3, p. 84, 1969.
10. Martin, M.K., and Heywood, J.B., "Approximate Relationships for the Thermodynamic Properties of Hydrocarbon-Air Combustion Products," to be published in *Combustion Science and Technology*.

11. Babkin, V.S. and Kozachenko, L.S., "Study of Normal Burning Velocity in Methane-Air Mixtures at High Pressures," *Combustion, Explosion, and Shock Waves*, 2, 77-86 (1966).
12. Heimel, S. and Weast, R., "Effect of Initial Mixture on the Burning Velocity of Benzene-Air, n-Heptane-Air, and Isooctane-Air Mixtures", Sixth Symposium (International) on Combustion p. 296.
13. Gibbs, G.J. and Calcote, H.F., *J. Chem. Eng. Data* 4, 226-237 (1959).
14. Rallis, et al, "The Determination of Burning Velocities of Normal Combustion Flame in a Spherical Constant Volume Vessel" *the South African Mechanical Engineer* March 1962 p. 233.
15. Andrews, G.E. and Bradley, D., *Combustion and Flame*, 18, 133-153 (1972).
16. DeSoete, G.G., "The Influence of Isotropic Turbulence on the Critical Ignition Energy", Thirteenth Symposium on Combustion p. 735.
17. Agnew, J.T. and Graiff "The Pressure Dependence of Laminar Burning Velocity by the Spherical Bomb Method" *Combustion and Flame* (September 1961) p. 209.
18. Andrews, G.E. and Bradley, D., *Combustion and Flame* 19, 275-288 (1972).
19. Bradley, D. and Hundy, G.F., "Burning Velocities of Methane-Air Mixtures Using Hot-Wire Anemometers in Closed-Vessel Explosions", Thirteenth Symposium on Combustion p. 575.
20. Gardner et al "Effect of Pressure on Burning Velocities of Benzene-Air, n-Heptane-Air, and 2, 2, 4- Trimethylpentane-Air Mixtures *Fuel* 30, (1950).
21. Strauss, W.A. and Edse, R. "Burning Velocity Measurements by The Constant-Pressure Bomb Method" Seventh Symposium on Combustion (1959) p. 56.
22. Smoot et al, *Combustion and Flame* 26, 323-342 (1976).

23. Nair, M.R.S., and Budta, M.C., *Combustion and Flame* 22, 219-221 (1974).
24. Manton et al "Burning-Velocity Measurements in a spherical Vessel with Central Egnition" Fourth Symposium on Combustion (1953)
25. Smith, D. and Agnew, J., "The Effect of Pressure on the Laminar Burning Velocity of Methane-Oxygen-Nitrogen Mixtures" Sixth Symposoum on Combustion (1957)
26. Escmenbach, R.C. and Agnew, J.T., *Combustion and Flame* 2, 273-285 (1958).
27. Blizard, N.C. and Keck, J.C., "Experimental and Theoretical Investigation of Trubulent Burning Model for Internal Combustion Engines" paper 740191 presented at Automotive Engineering Congress, Detroit, February 1974.
28. Ferguson, C.R. and Keck, J.C., "On Laminar Flame Quenching and Its Application to Engine Combustion", to be published in *Combustion and Flame*.
29. Lewis and VonElbe, "Combustion, Flames and Explosions of Gases".

TABLE IV

Parameters S_{uo} , α, β, ϵ , and their r.m.s. Fluctuations for Methane-Air Mixtures

ϕ	$S_{uo} \pm \Delta S_{uo}$	$\alpha \pm \Delta\alpha$	$\beta \pm \Delta\beta$	$\epsilon \pm \Delta\epsilon$
0.8	29.5±0.94	1.53±0.09	-0.38±0.01	0.17±0.01
0.9	34.36±2.92	0.34±10.69	0.10±4.04	0.23±0.01
1.0	35.86±.77	1.29±0.06	-0.26±0.01	0.19±0.01
1.05	39.43±2.09	-8.46±7.05	3.35±2.61	0.20±0.01
1.1	34.59±3.58	2.53±11.76	-0.72±4.33	0.22±0.01
1.2	31.32±1.09	1.52±0.10	-0.38±0.01	0.19±0.02
1.3	22.04±1.73	1.92±4.60	-0.52±1.68	0.18±0.02

TABLE V

Parameters S_{uo} , α , β , ϵ , and their r.m.s. Fluctuations for Isooctane-Air Mixtures

ϕ	$S_{uo} \pm \Delta S_{uo}$	$\alpha \pm \Delta\alpha$	$\beta \pm \Delta\beta$	$\epsilon \pm \Delta\epsilon$
0.7	33.78 \pm 1.34	2.75 \pm 0.13	-0.59 \pm 0.02	0.34 \pm 0.01
0.8	33.43 \pm 1.52	2.41 \pm 0.14	-0.36 \pm 0.03	0.42 \pm 0.02
0.9	33.53 \pm 1.21	-18.07 \pm 10.67	6.54 \pm 3.36	0.45 \pm 0.01
1.0	35.25 \pm 1.33	1.85 \pm 0.13	-0.12 \pm 0.02	0.45 \pm 0.01
1.05	30.97 \pm 1.28	-1.58 \pm 9.71	1.02 \pm 3.24	0.50 \pm 0.01
1.1	29.68 \pm 1.31	16.39 \pm 13.11	-4.95 \pm 4.32	0.44 \pm 0.01
1.2	27.63 \pm 1.04	1.30 \pm 0.14	0.05 \pm 0.03	0.46 \pm 0.01
1.3	22.25 \pm 1.02	9.18 \pm 9.46	-2.46 \pm 3.12	0.48 \pm 0.01
1.4	17.14 \pm 0.8	14.14 \pm 8.24	-3.98 \pm 2.78	0.52 \pm 0.01
1.5	13.49 \pm 0.87	43.48 \pm 11.05	-13.33 \pm 3.62	0.33 \pm 0.02
1.6	11.19 \pm 0.54	69.28 \pm 11.38	-21.43 \pm 3.57	0.15 \pm 0.02

TABLE VI

Parameters S_{uo} , α, β, ϵ , and their r.m.s. Fluctuations for Methanol-Air Mixture

ϕ	$S_{uo} \pm \Delta S_{uo}$	$\alpha \pm \Delta\alpha$	$\beta \pm \Delta\beta$	$\epsilon \pm \Delta\epsilon$
0.7	24.48±1.09	2.37±0.20	-0.41±0.05	0.43±0.01
0.8	31.72±2.09	2.12±0.30	-0.28±0.07	0.45±0.02
0.9	45.37±0.02	-2.50±9.18	1.29±3.22	0.42±0.01
1.0	44.32±1.48	-16.30±7.55	6.05±2.60	0.50±0.01
1.05	44.11±2.13	-15.82±10.74	5.87±3.79	0.45±0.01
1.1	40.69±1.29	-14.85±5.54	5.57±1.90	0.50±0.01
1.2	40.80±1.14	13.56±5.18	-4.13±1.77	0.47±0.01
1.3	36.05±1.43	-30.75±9.55	10.86±3.23	0.54±0.01
1.4	46.89±8.38	-18.45±7.67	6.64±2.56	0.20±0.01
1.5	19.95±3.97	11.65±8.99	-3.37±2.93	0.65±0.01

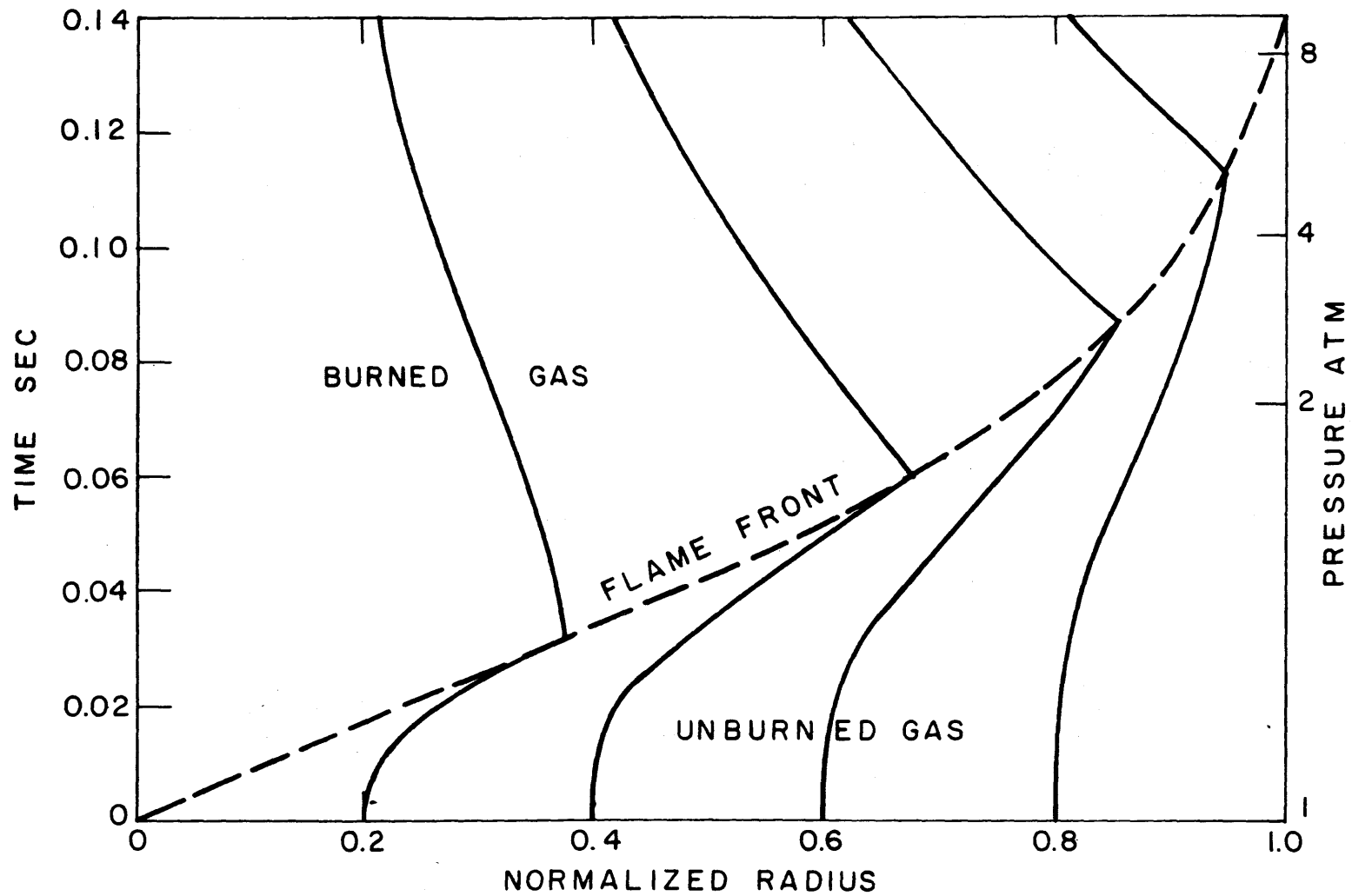


Figure 1: Particle Trajectories of Stoichiometric Methane-Air Mixture with Initial Conditions of $P_i = 1$ ATM and $T_i = 300^\circ\text{k}$ Having Constant Burning Velocity ($S_u = \text{Const.} = 1$).

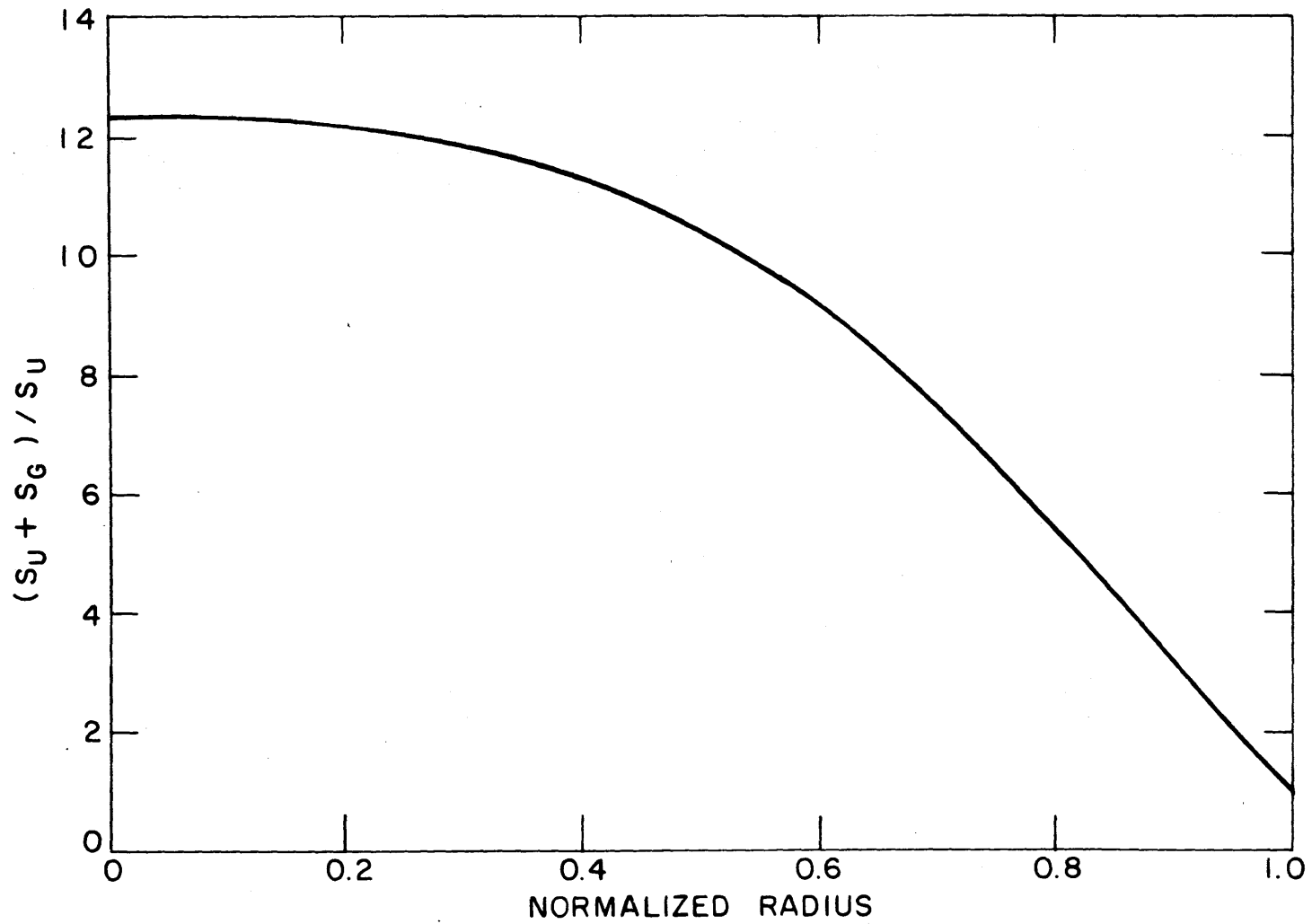
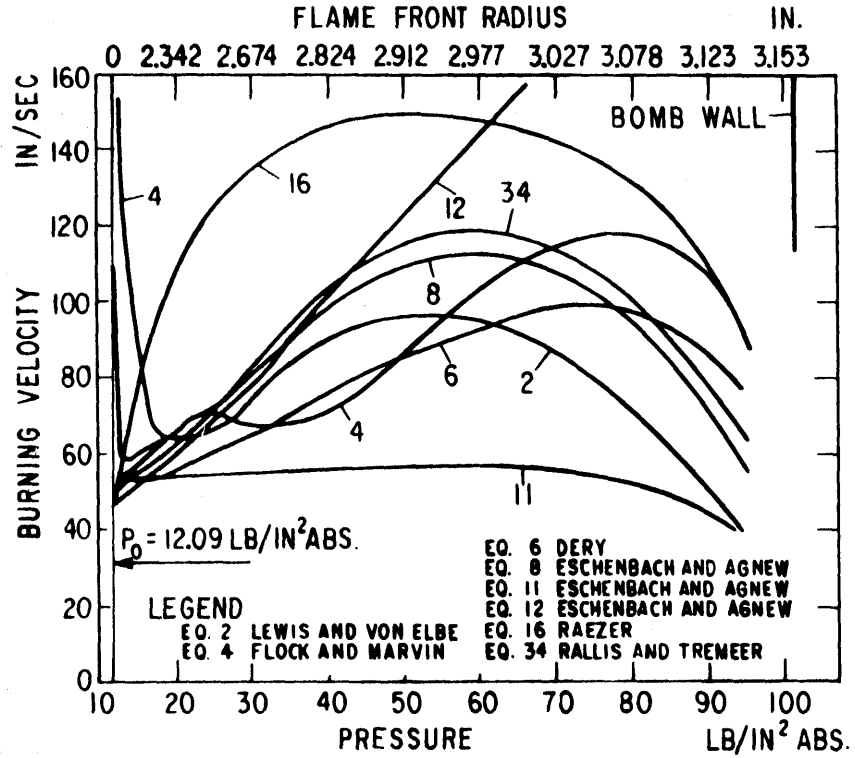
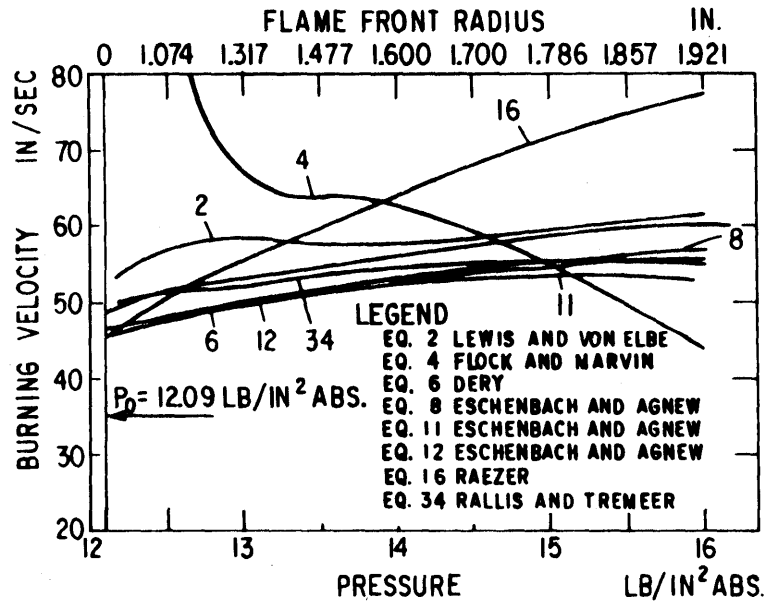


Figure 2: Flame Speed Versus Burning Velocity for Stoichiometric Methane-Air Mixture with Initial Condition of $P_i = 1$ ATM and $T_i = 300^\circ\text{k}$.



COMPARISON OF BURNING VELOCITY EQUATIONS FOR A STOICHIOMETRIC ACETYLENE-AIR MIXTURE



COMPARISON OF BURNING VELOCITY EQUATIONS FOR A STOICHIOMETRIC ACETYLENE-AIR MIXTURE BASED ON LOW RANGE PRESSURE RECORDS

Figure 3: Comparison of Burning Velocity Equations.

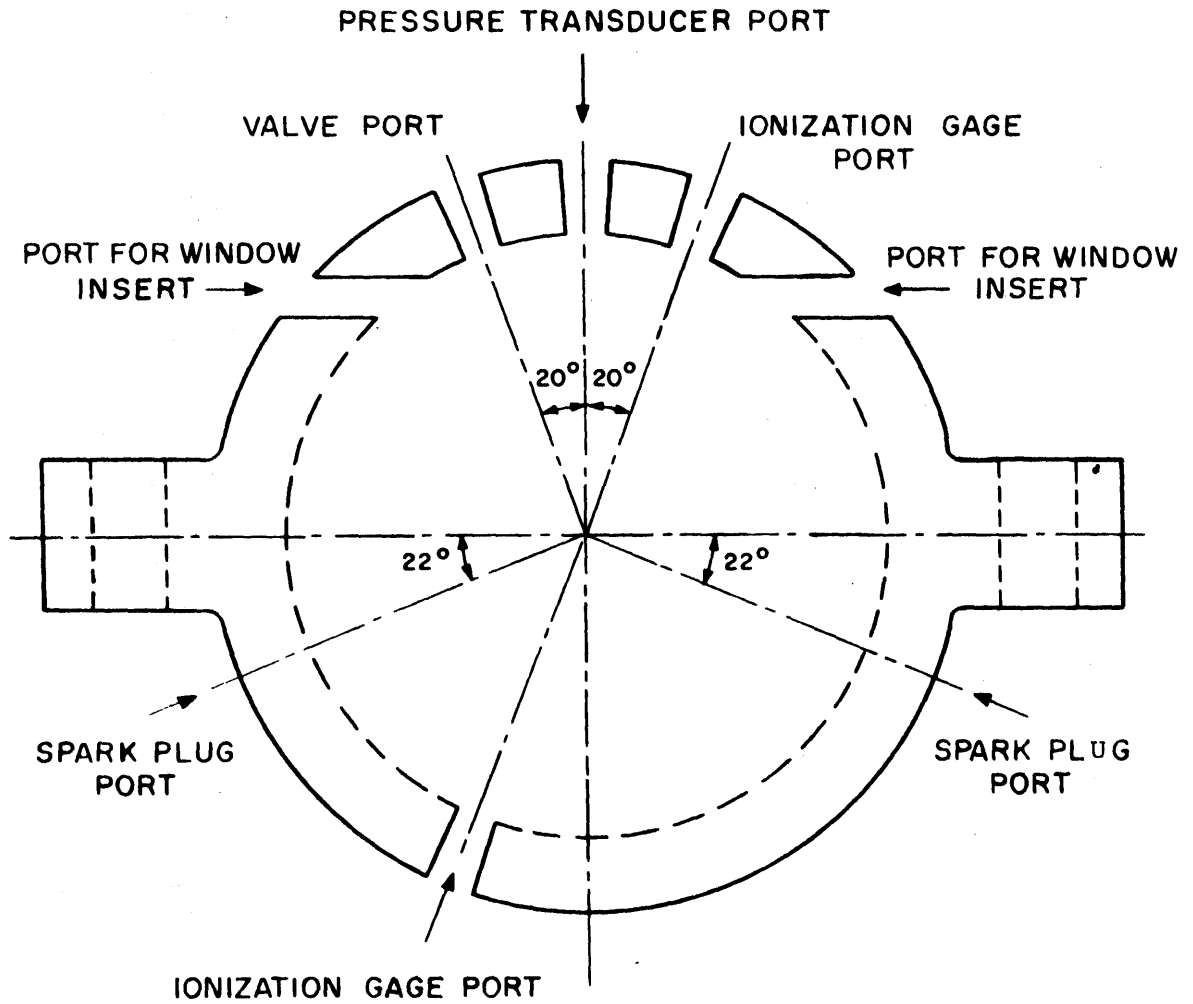


Figure 4: Schematic Diagram of the Combustion Bomb
(Third Ionization Gage Port is Behind Valve
Port).

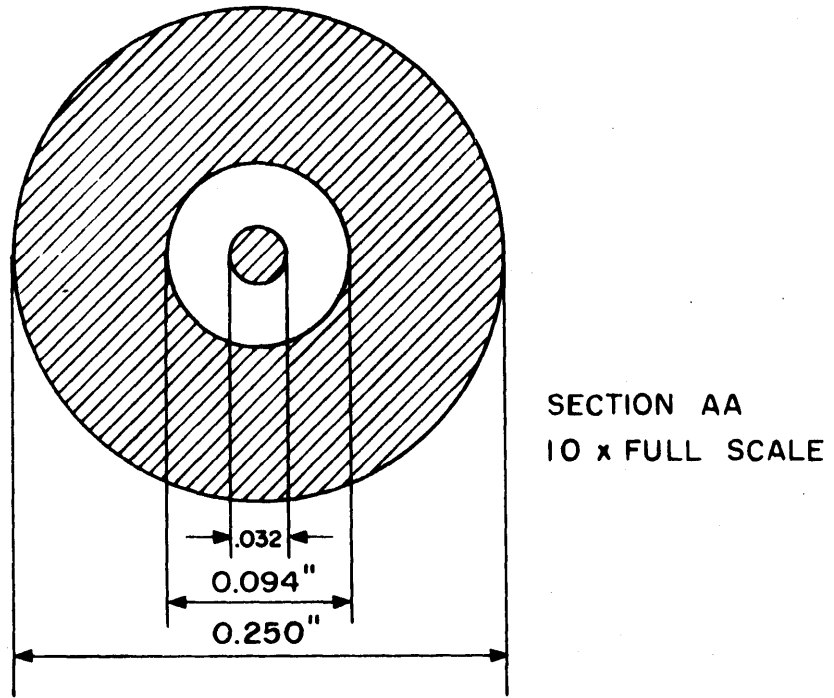
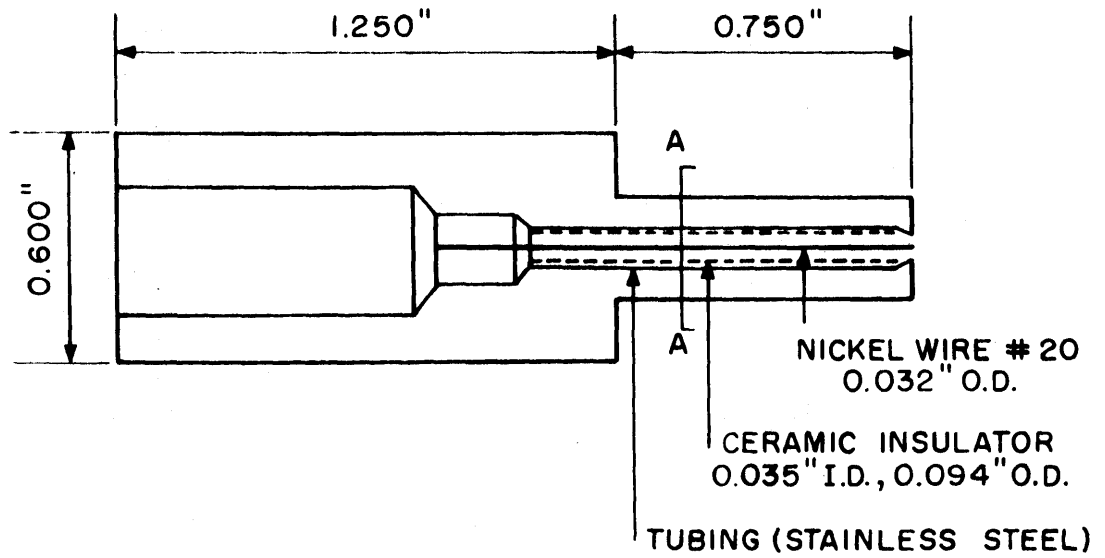


Figure 5: Schematic Diagrams Showing Construction of Ionization Probes.

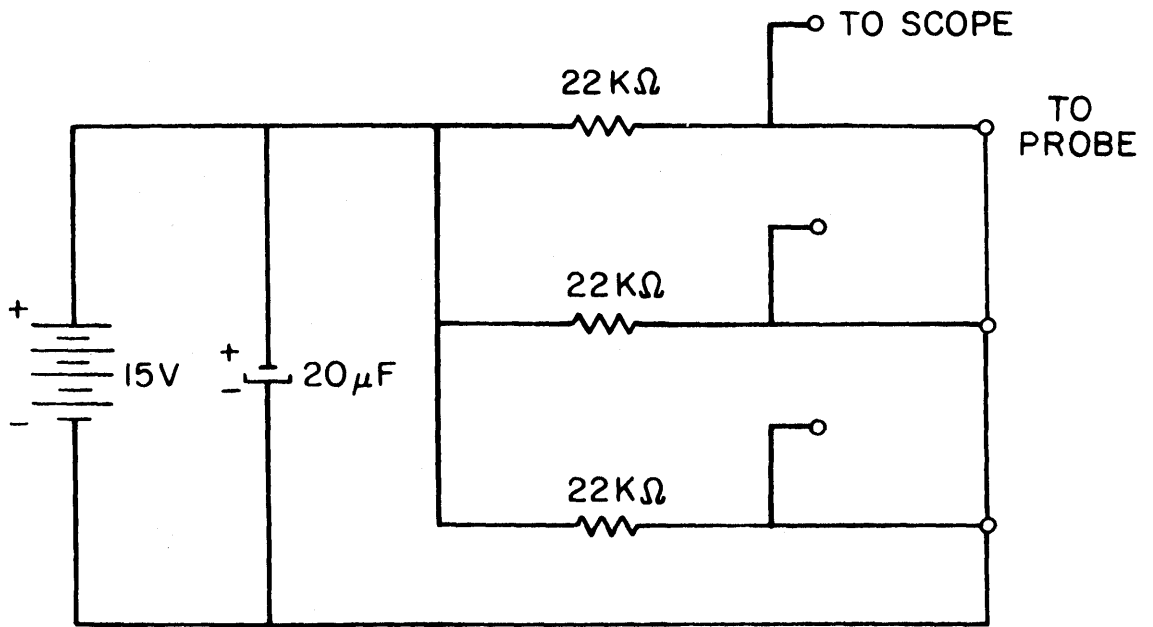


Figure 6: Schematic Diagrams of Ionization Probe Circuit.

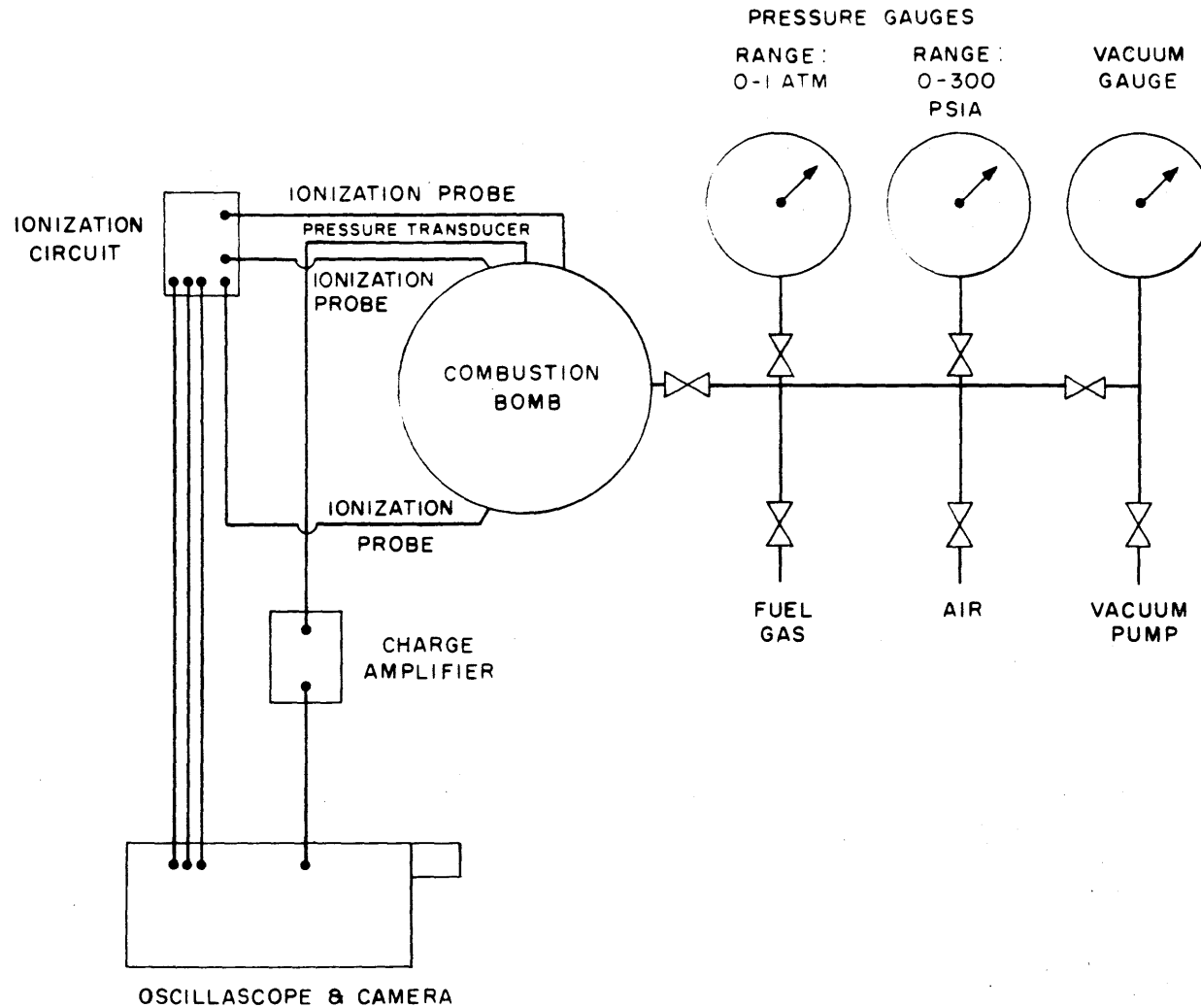


Figure 7: Schematic Diagram of Experimental Apparatus.

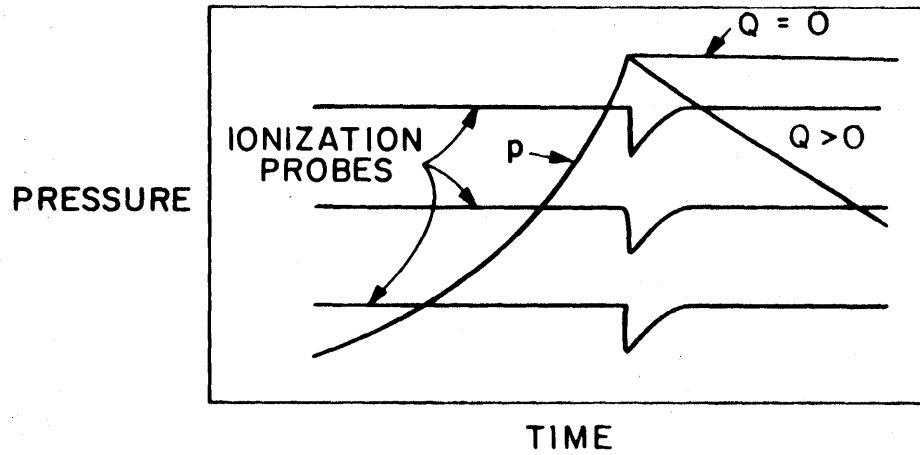


Figure 8: Ideal Pressure-Time Diagram and Ionization Probe Signals. Horizontal Curves: Ionization Probe Signals, and the Other Curve: Pressure-Time Diagram.

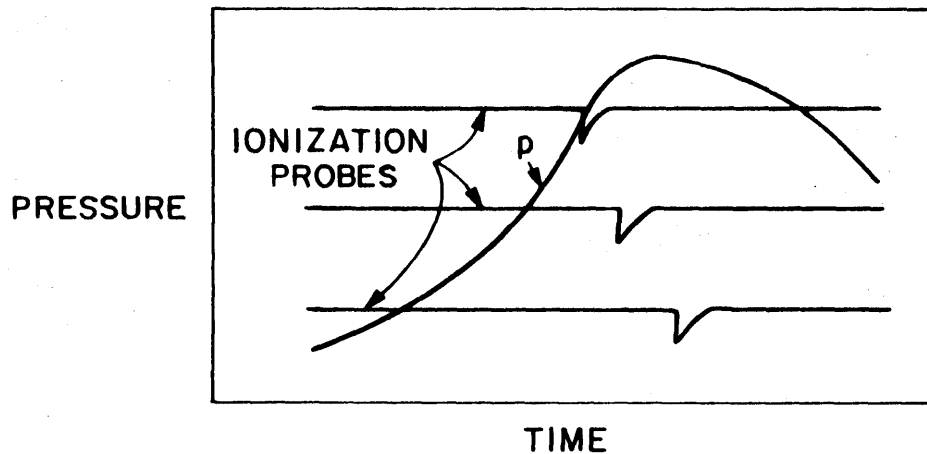


Figure 9: Pressure-Time Diagram and Ionization Probe Signals If Air-Fuel Mixture is not Homogeneous or the Electrodes are not at the Center of the Combustion Bomb.

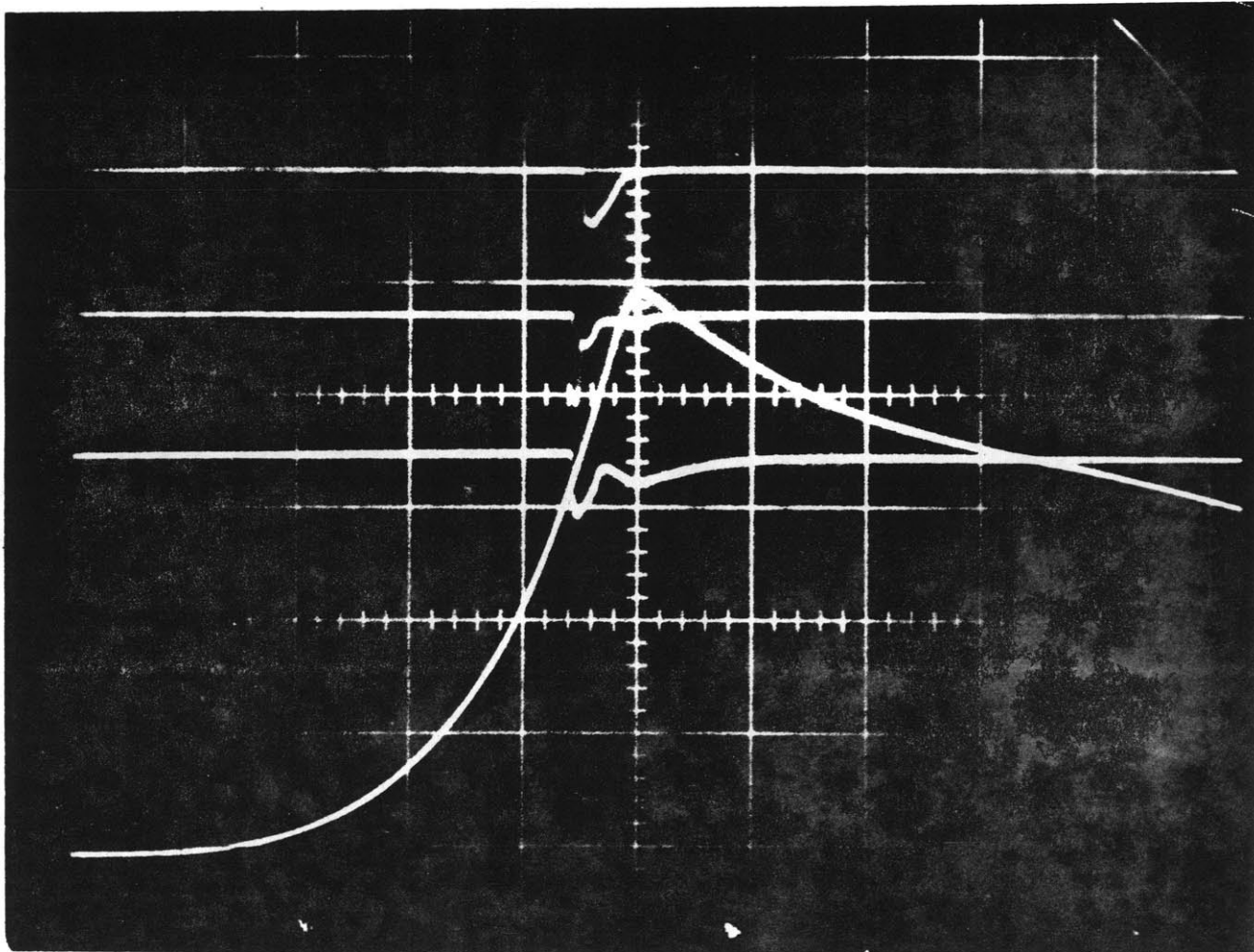


Figure 10 - Oscillogram for methane-air mixture at equivalence ratio of 0.9 and initial condition of $P_i=1$ ATM and $T_i=300^\circ\text{k}$ (vertical scale is 1.36 ATM/Div, and horizontal scale is 10 MSEC/Div).

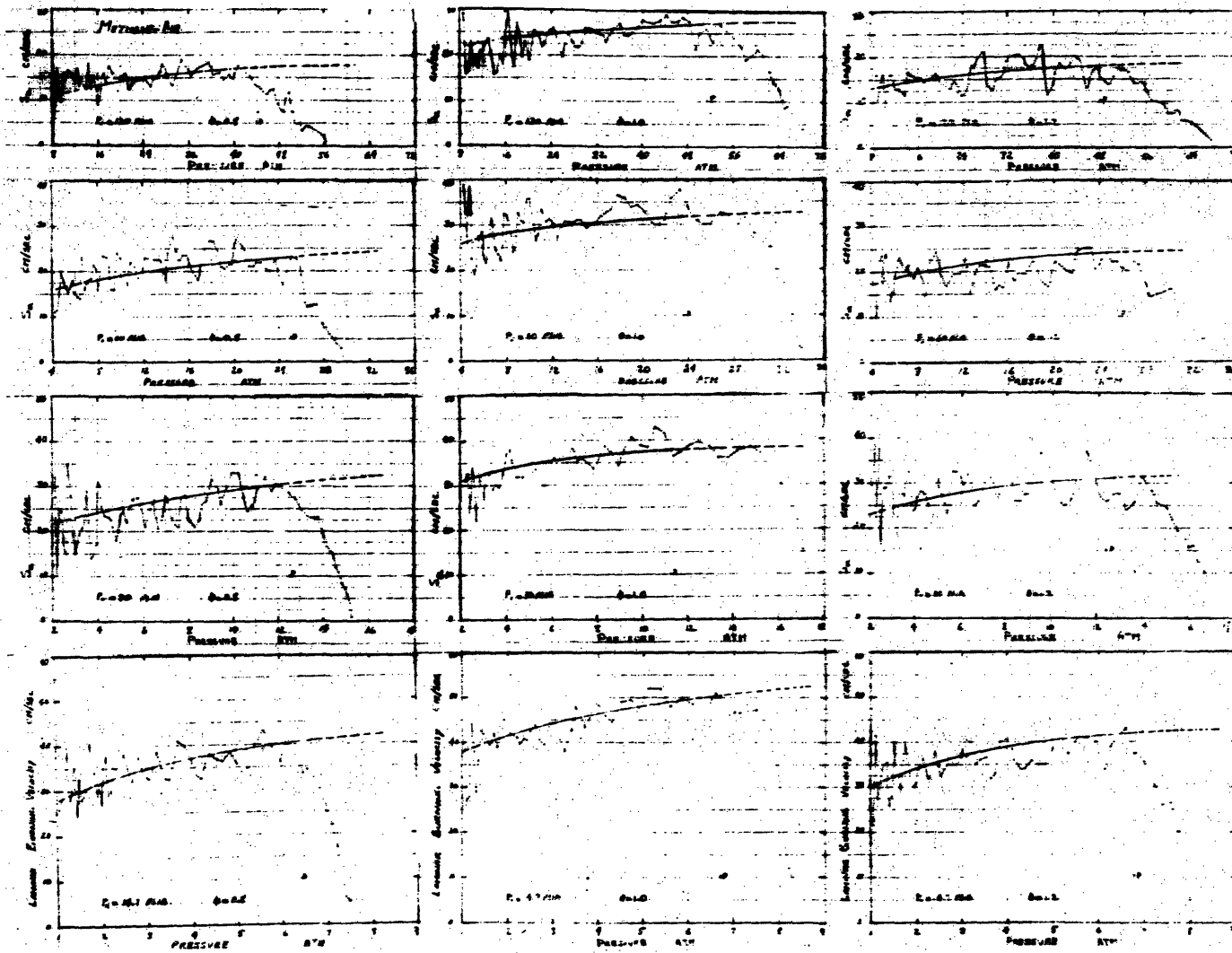


Figure 11: Measured and Fitted Burning Velocity of Methane-Air Mixtures at Equivalence Ratio of 0.8, 1.0, and 1.2 with Initial Temperature of 300°k and Four Different Initial Pressure of 1, 2.04, 3.06, and 4.08 ATM (Point "p" Represents Point of Discontinuity of Ionization Probes).

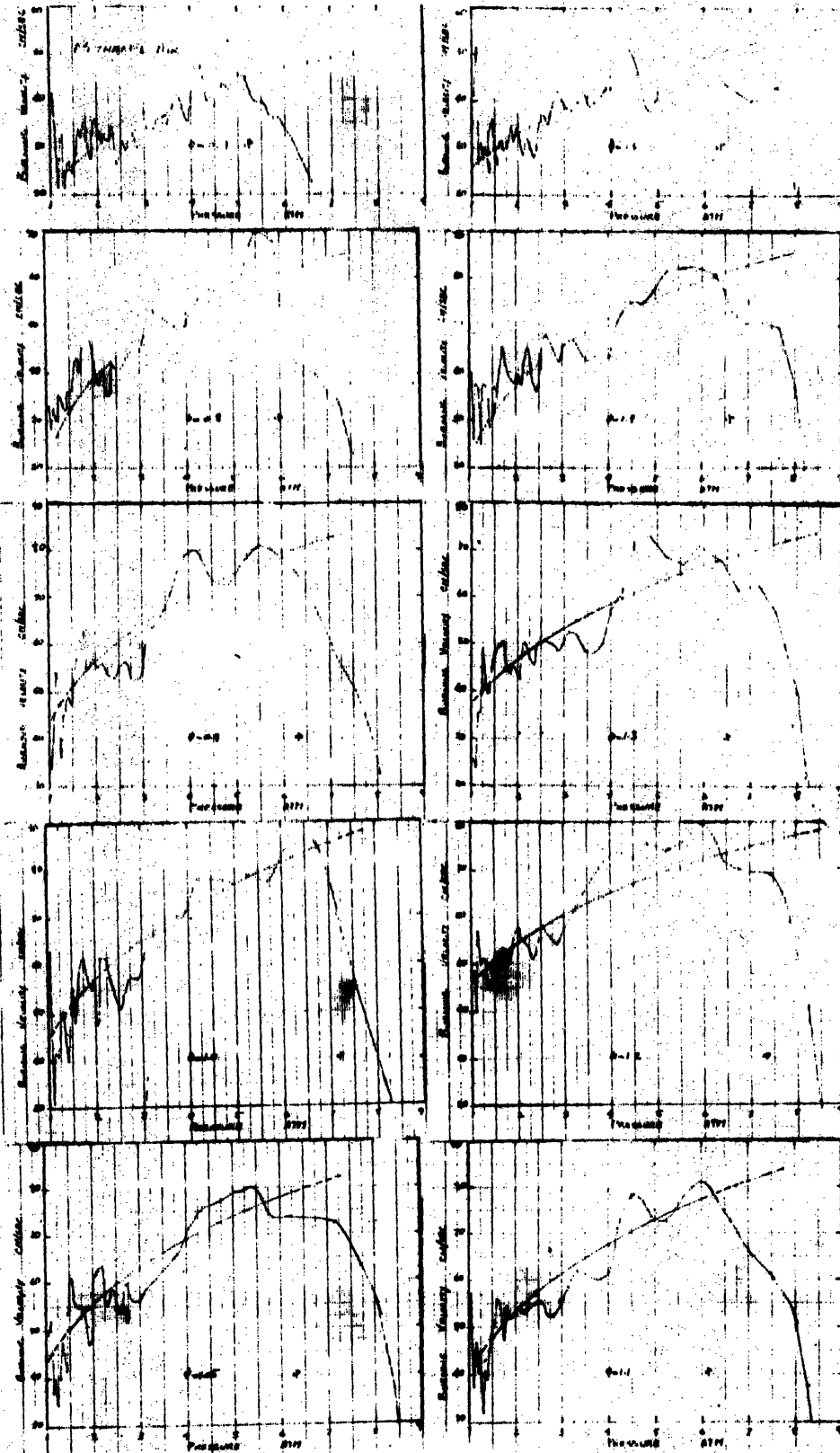


Figure 13: Measured and Fitted Burning Velocity of Methanol-Air Mixtures with Initial Temperature of 300°k and Initial Pressure of 1 ATM with Equivalence Ratio Ranging from 0.7 to 1.5. (Point "p" Represents Point of Discontinuity of Ionization Probes).

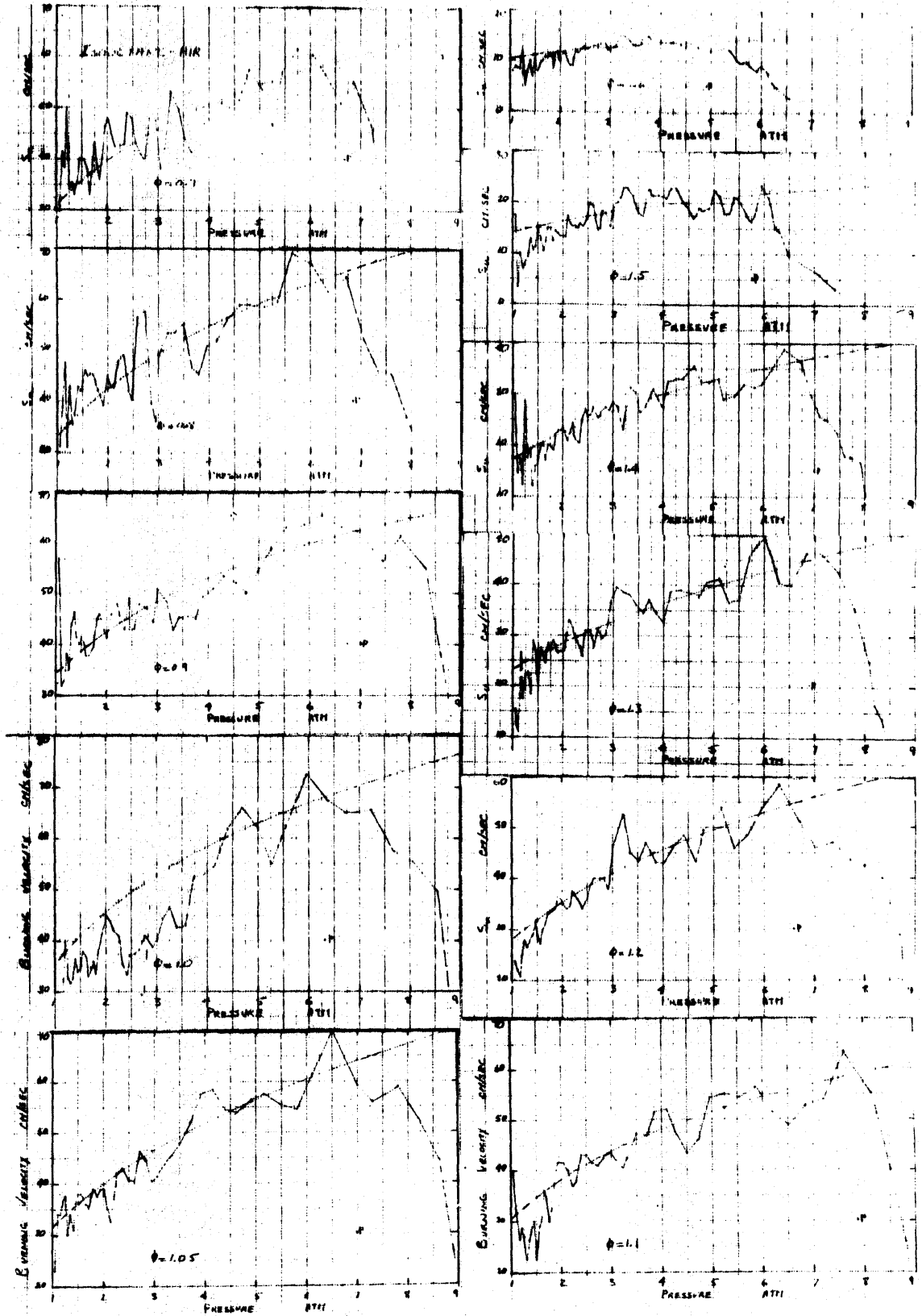


Figure 12: Measured and Fitted Burning Velocity of Isooctane-Air Mixtures with Initial Temperature of 300°k and Initial Pressure of 1 ATM with Equivalence Ratio Ranging from 0.7 to 1.6. (Point "p" Represents Point of Discontinuity of Ionization Probes).

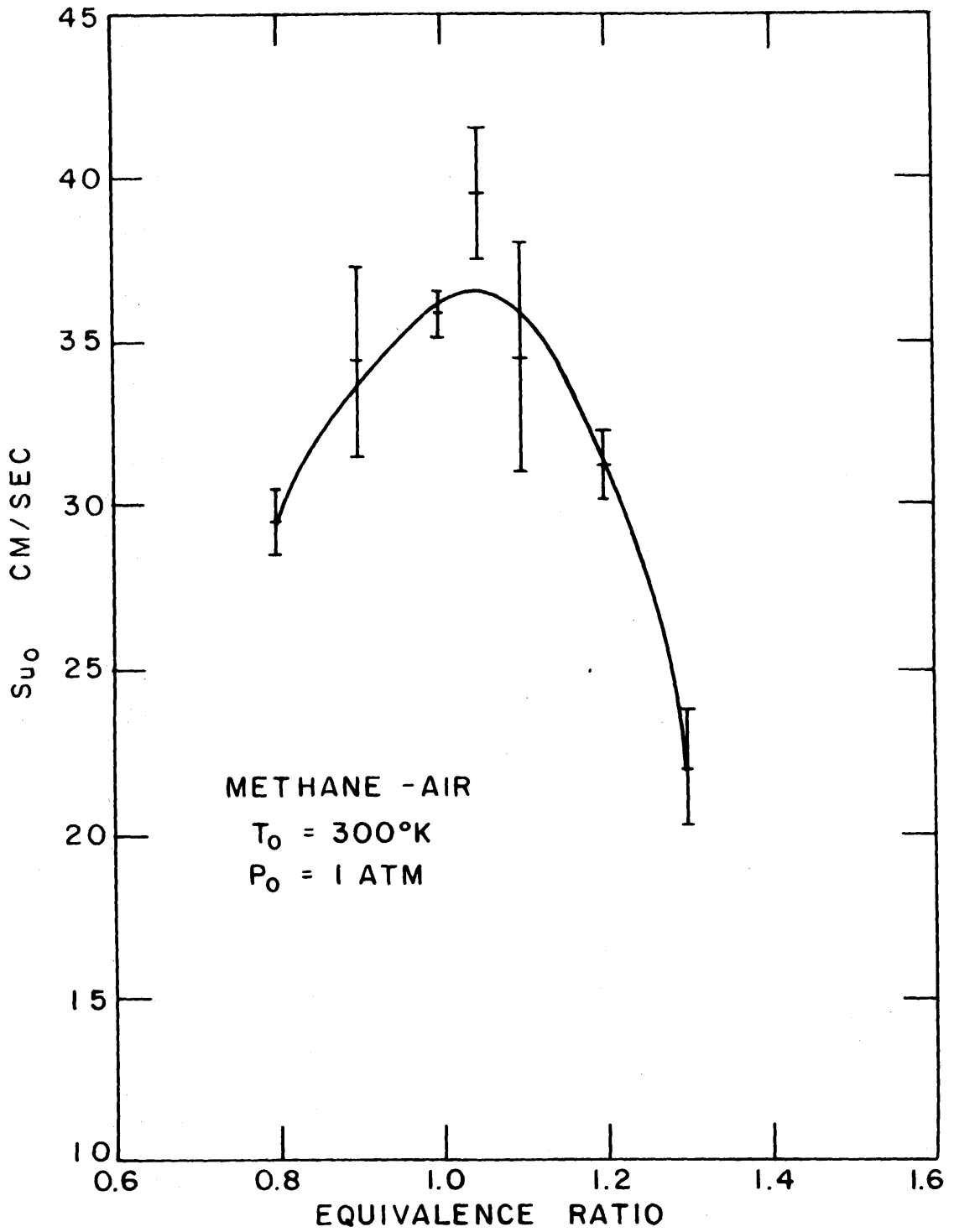


Figure 14: S_{uo} as a Function of Equivalence Ratio for Methane-Air Mixtures ($T_0 = 300^\circ\text{K}$, $P_0 = 1 \text{ ATM}$), Errors are Shown and the Curve is the Least Square Fit of 4th Order Polynomial.

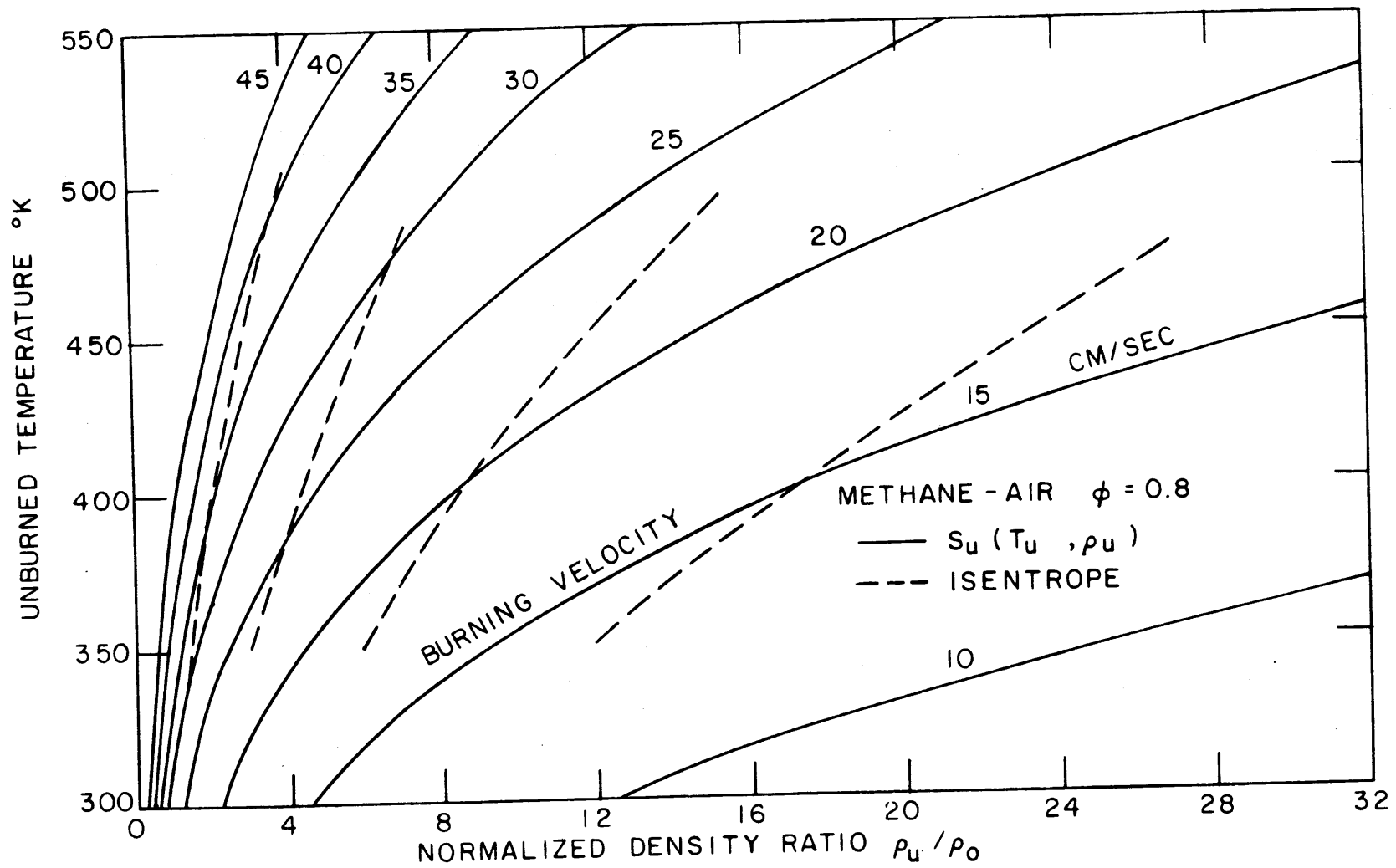


Figure 15: Contour Plot of Burning Velocity, Unburned Gas Temperature, and Normalized Unburned Density for Methane-Air Mixture at Equivalence Ratio of 0.8 ($P_0 = 1 \text{ ATM}$, $T_0 = 300^\circ\text{K}$).

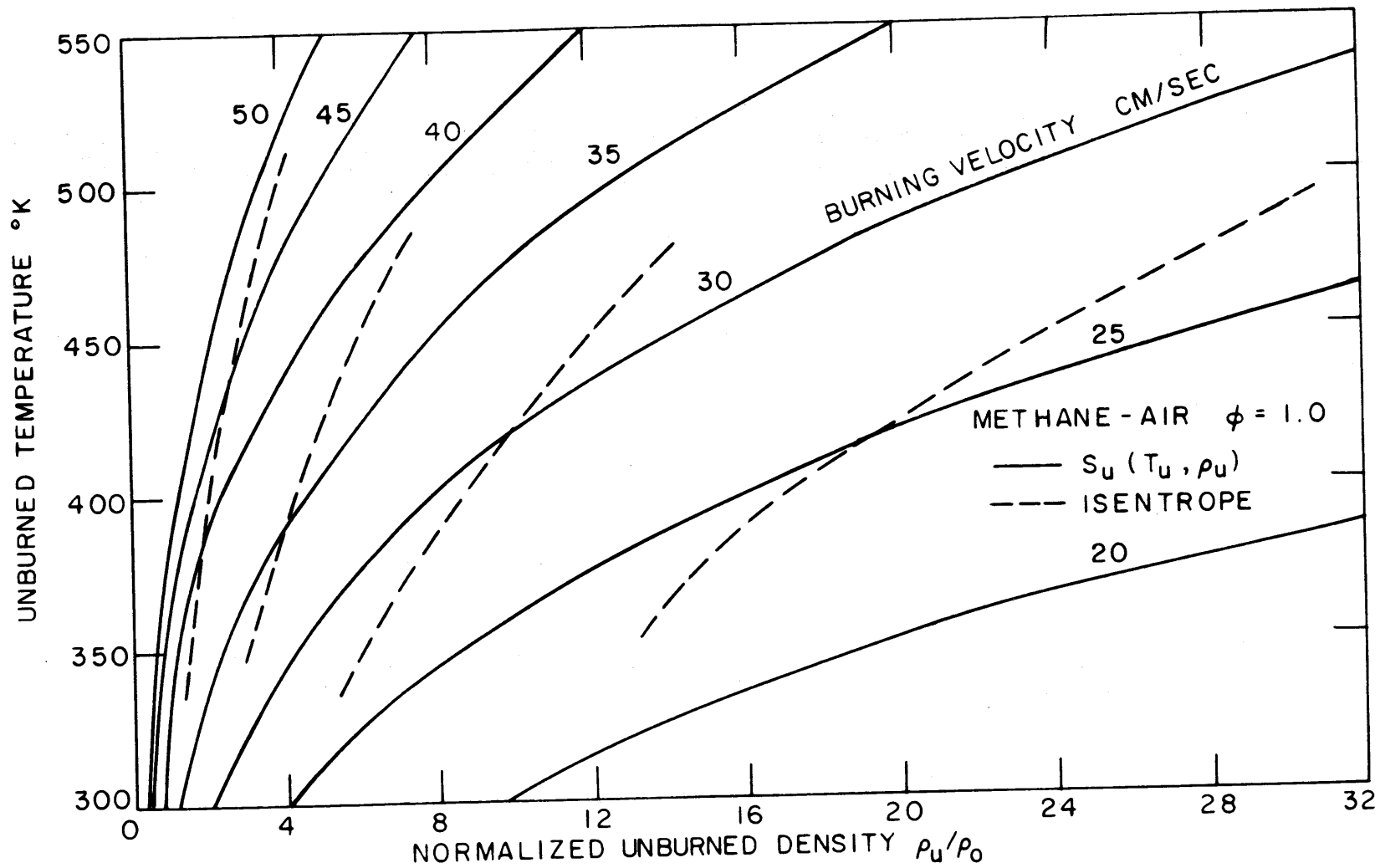


Figure 16: Contour Plot of Burning Velocity, Unburned Gas Temperature, and Normalized Unburned Density for Stoichiometric Methane-Air Mixture ($P_0 = 1 \text{ ATM}$, $T_0 = 300^{\circ}\text{K}$).

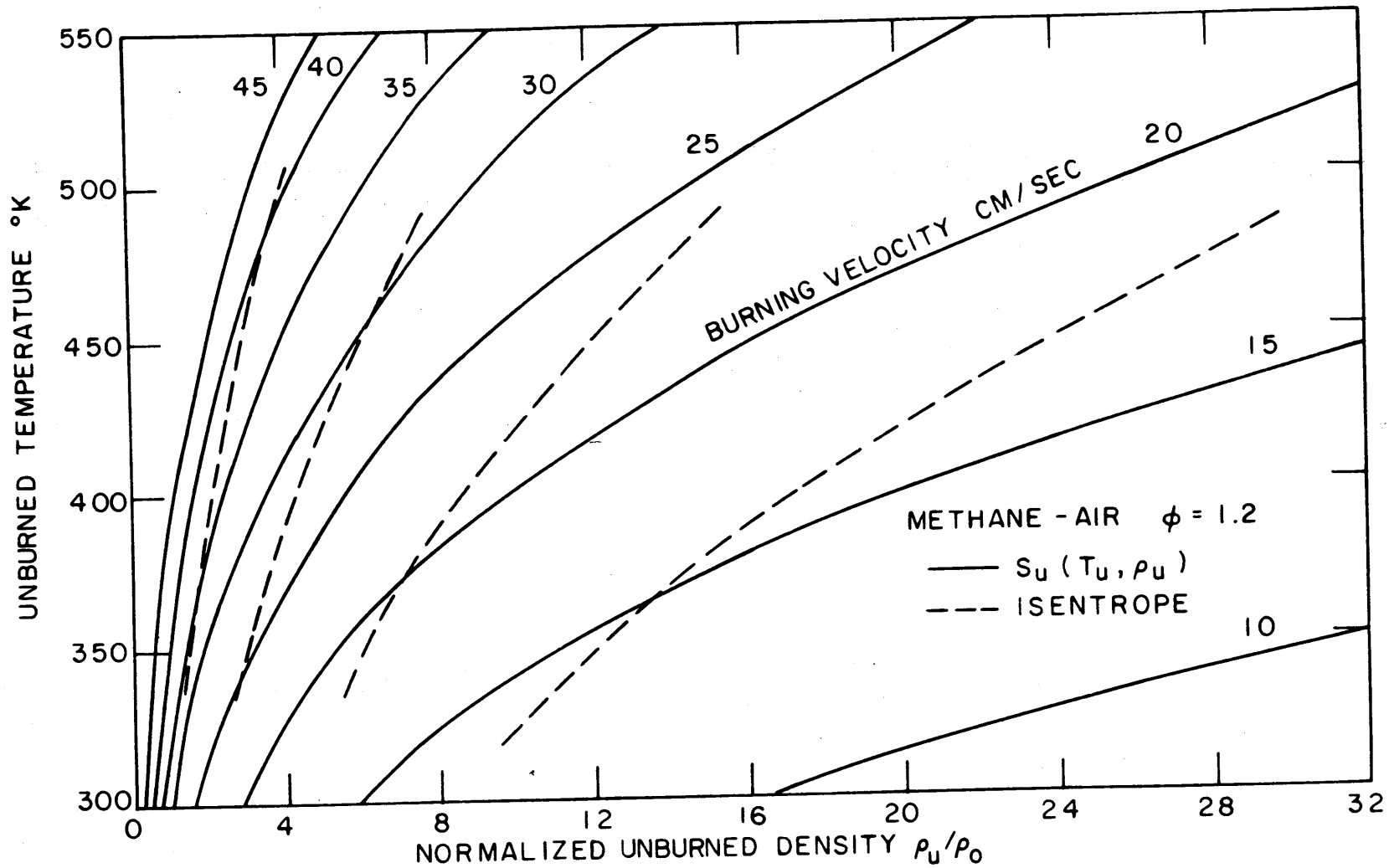


Figure 17: Contour Plot of Burning Velocity, Unburned Gas Temperature, and Normalized Unburned Density for Methane-Air Mixture at Equivalence Ratio of 1.2 ($P_0 = 1 \text{ ATM}$, $T_0 = 300 \text{ K}$).

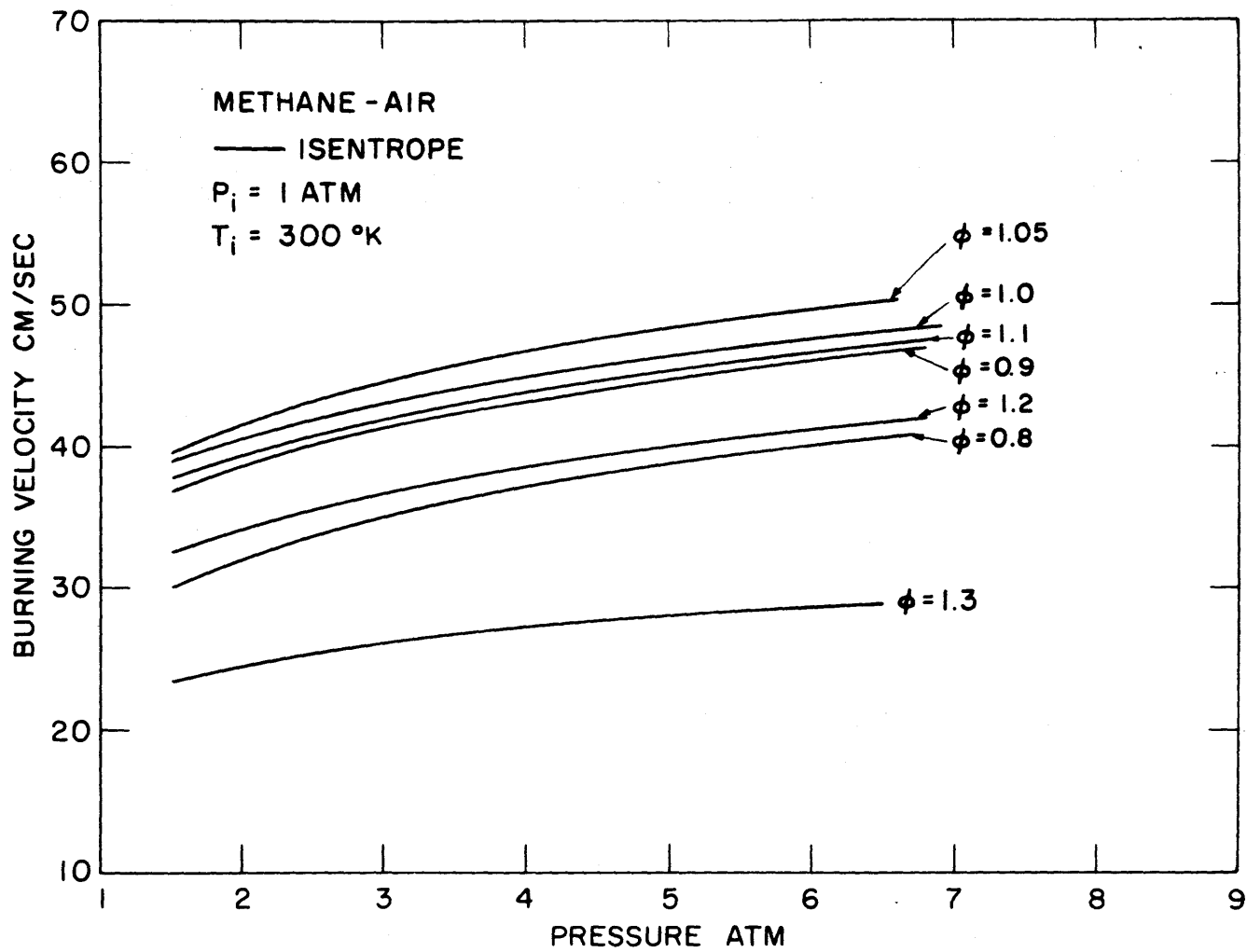


Figure 18: Burning Velocity for Isentropes of Methane-Air Mixtures at Different Equivalence Ratio ϕ as a Function of Pressure with Initial Condition of $T_i = 300^\circ\text{k}$.

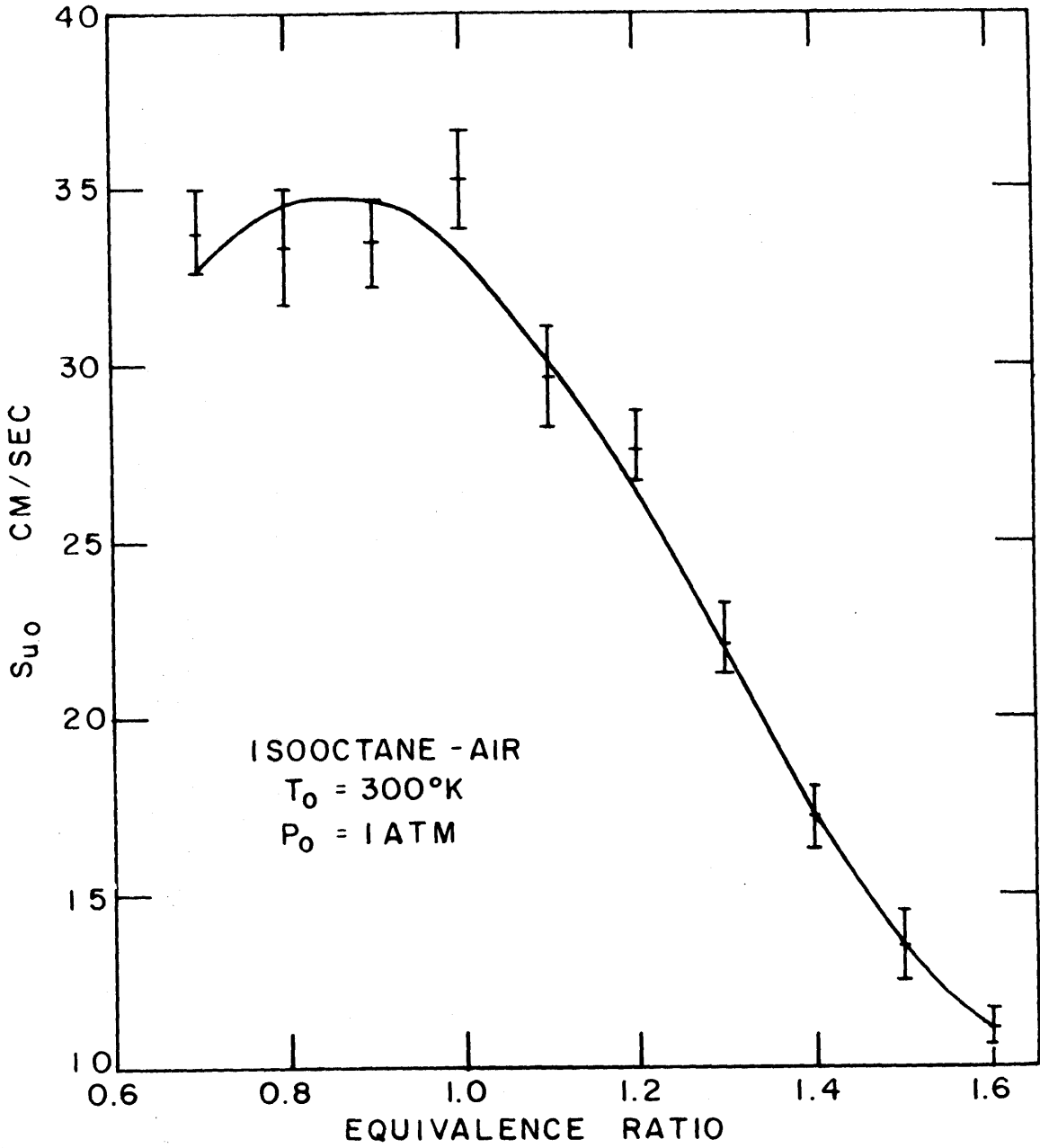


Figure 19: S_{uo} as a Function of Equivalence Ratio for Isooctane-Air Mixtures ($T_0 = 300^\circ\text{K}$, $P_0 = 1\text{ ATM}$), R.M.S. Errors are Shown and the Curve is the Least Square Fit of Third Order Polynomial.

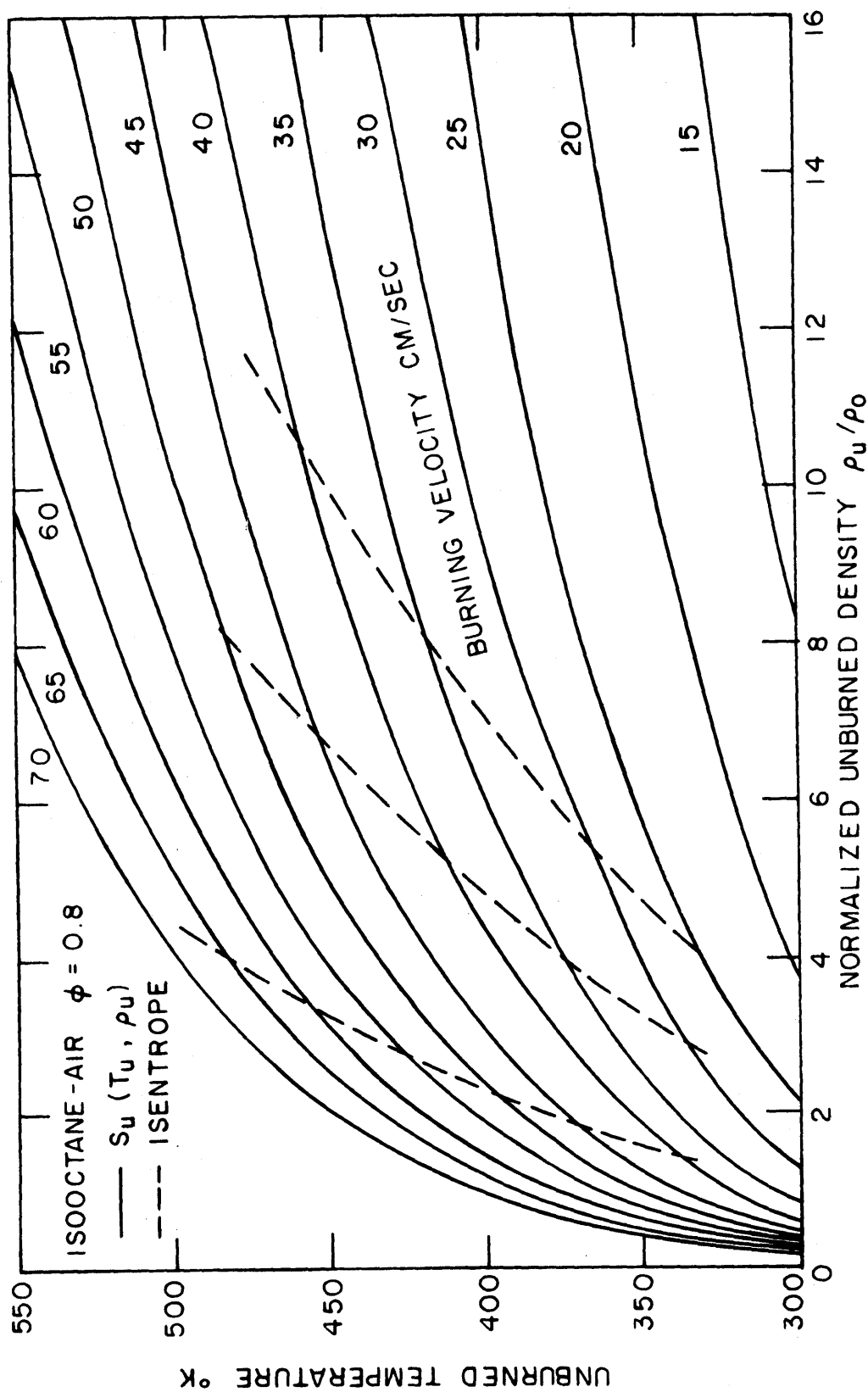


Figure 20: Contour Plot of Burning Velocity, Unburned Gas Temperature, and Normalized Unburned Density for Isooctane-Air Mixture at Equivalence Ratio of 0.8 ($P_0 = 1 \text{ ATM}$, $T_0 = 300^\circ\text{K}$).

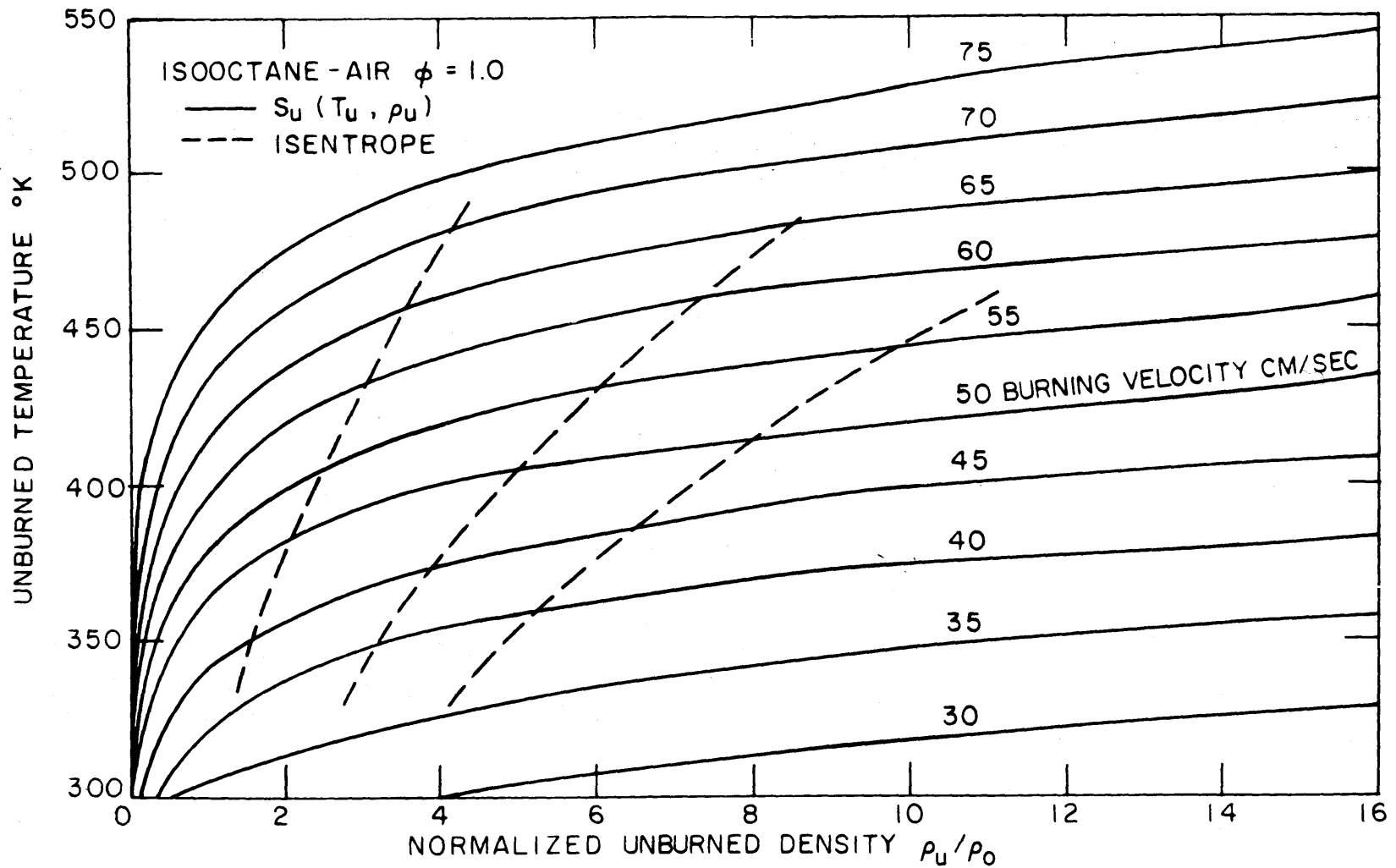


Figure 21: Contour Plot of Burning Velocity, Unburned Gas Temperature, and Normalized Unburned Density for Stoichiometric Isooctane-Air Mixture ($P_0 = 1 \text{ ATM}$, $T_0 = 300^\circ\text{K}$).

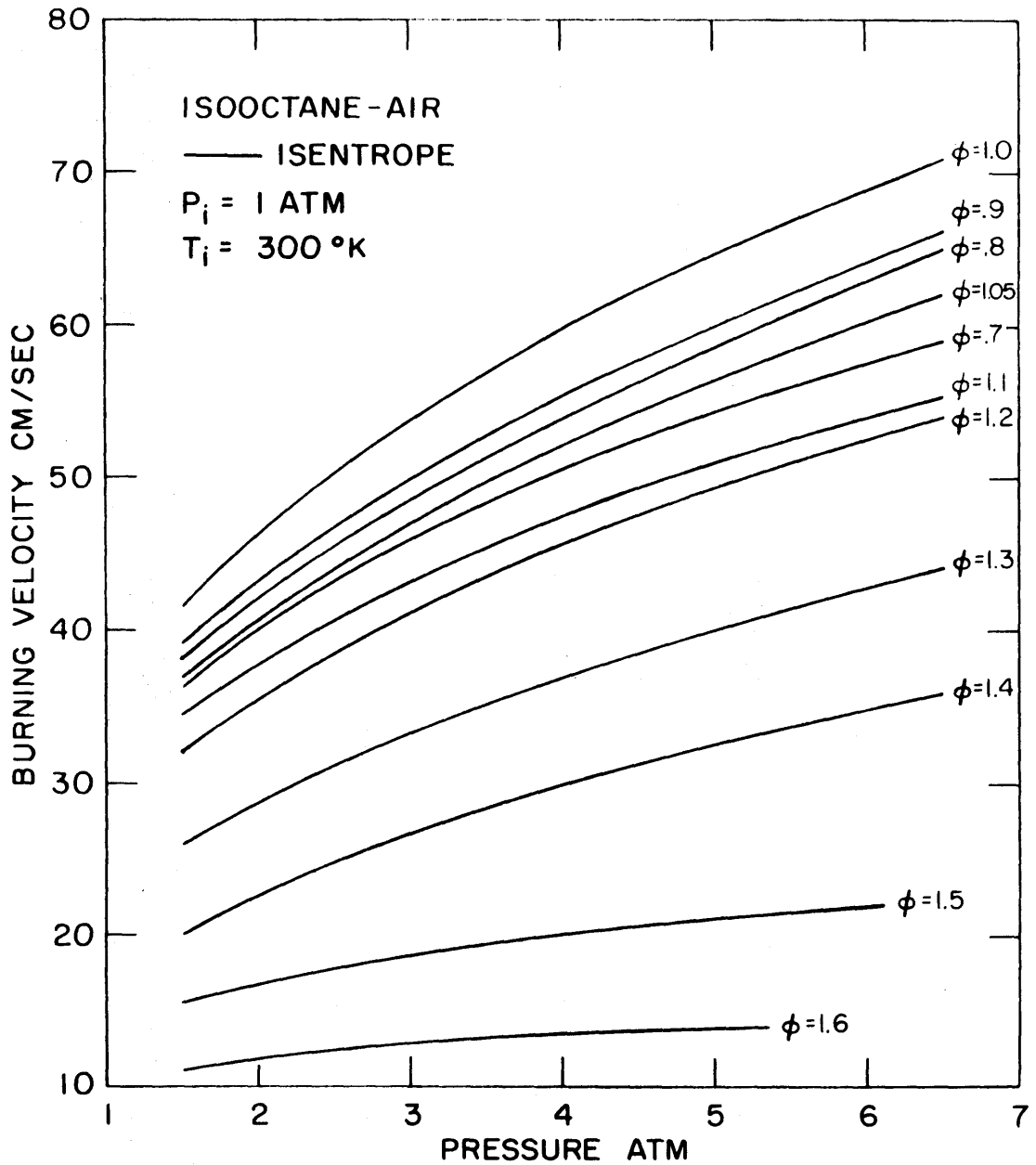


Figure 22: Burning Velocity of Isentropes of Isooctane-Air Mixtures at Different Equivalence Ratio ϕ as a Function of Pressure with Initial Condition of $T_i = 300^\circ\text{K}$, $P_i = 1 \text{ ATM}$.

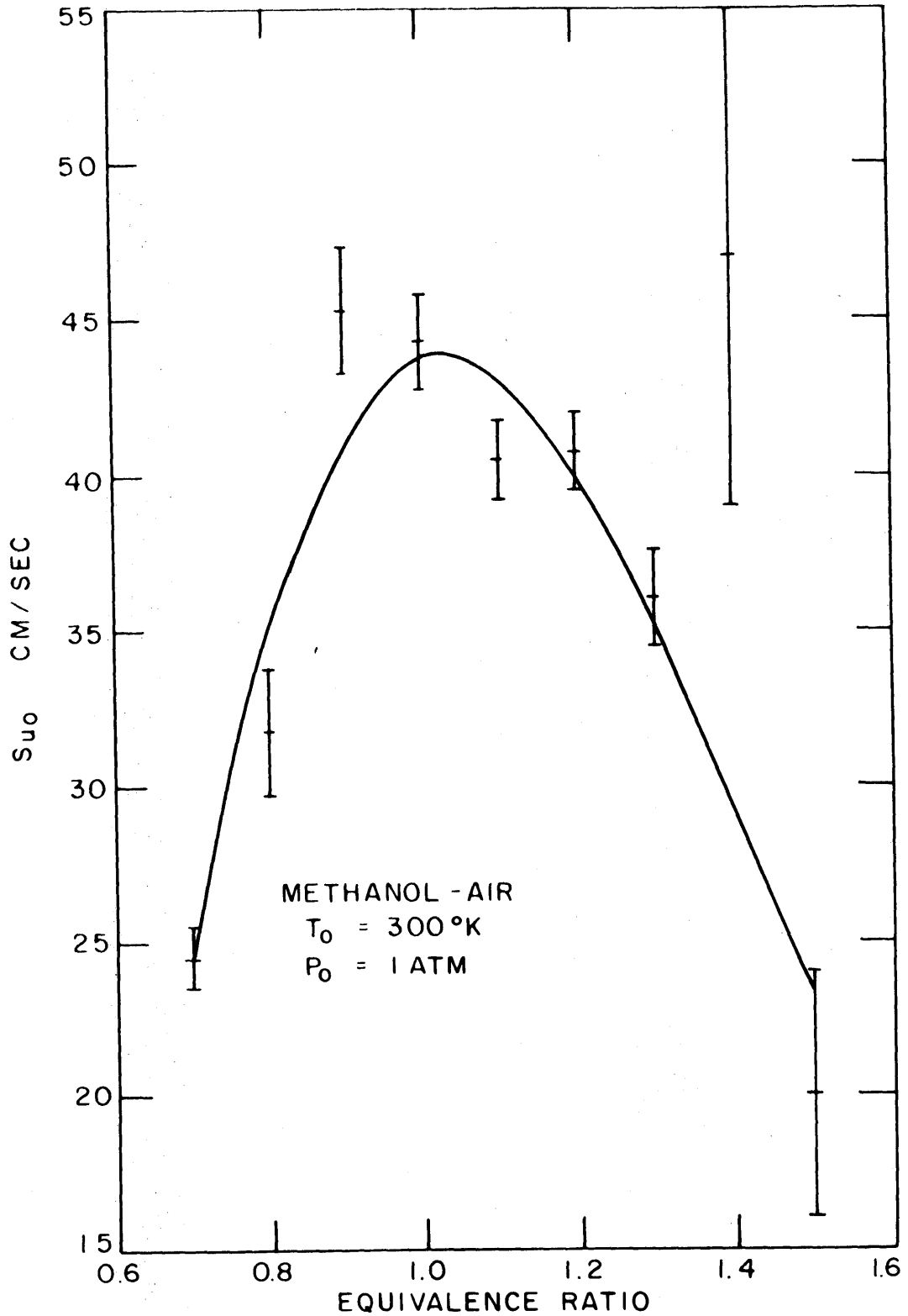


Figure 23: S_{uo} as a Function of Equivalence Ratio for Methanol-Air Mixtures ($T_0 = 300^\circ\text{K}$, $P_0 = 1 \text{ ATM}$), R.M.S. Errors are Shown, and the Curve is the Least Square Fit of 4th Order Polynomial.

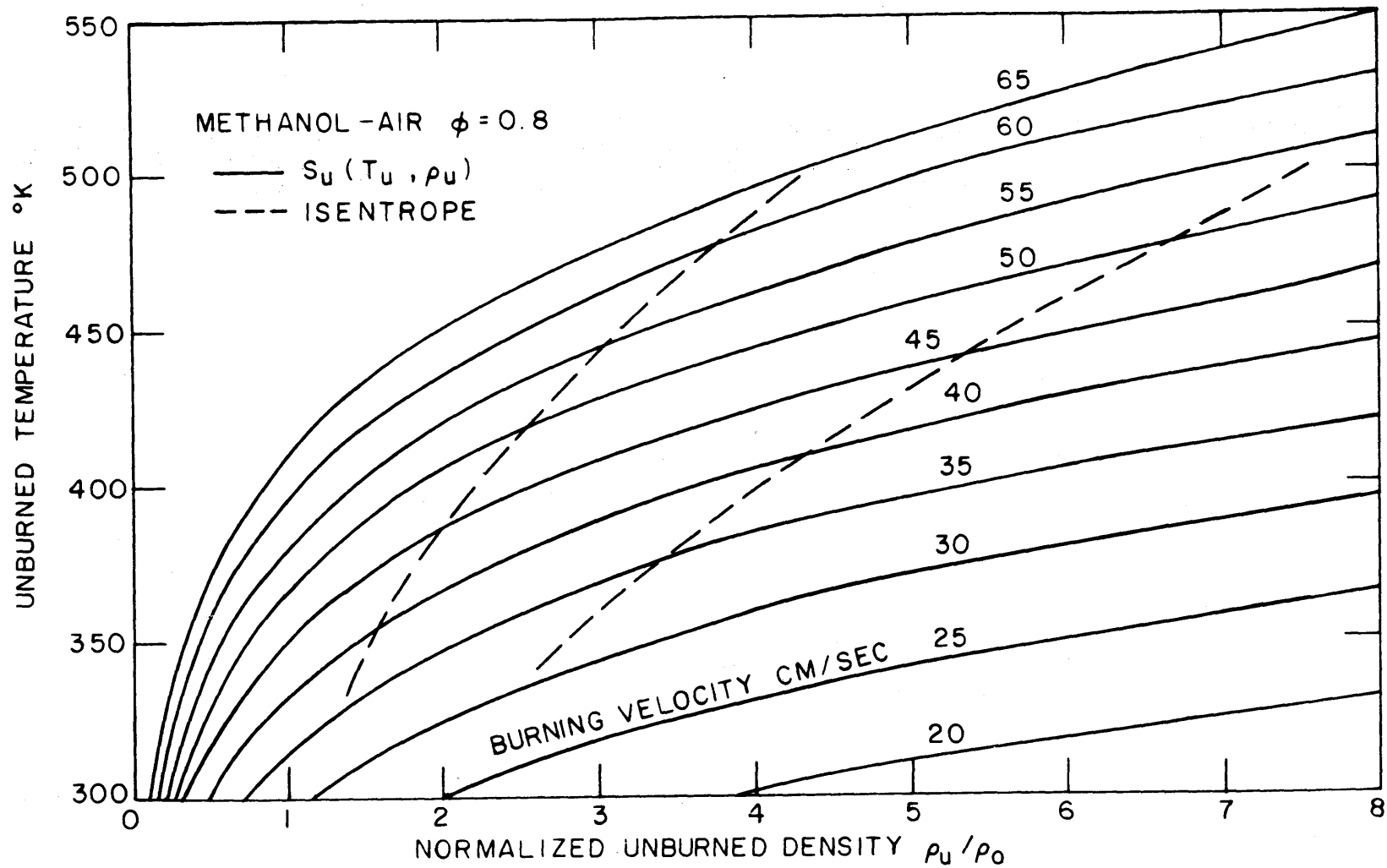


Figure 24: Contour Plot of Burning Velocity, Unburned Gas Temperature, and Normalized Unburned Density for Methanol-Air Mixture at Equivalence Ratio of 0.8 ($P_0 = 1 \text{ ATM}$, $T_0 = 300^\circ\text{K}$).

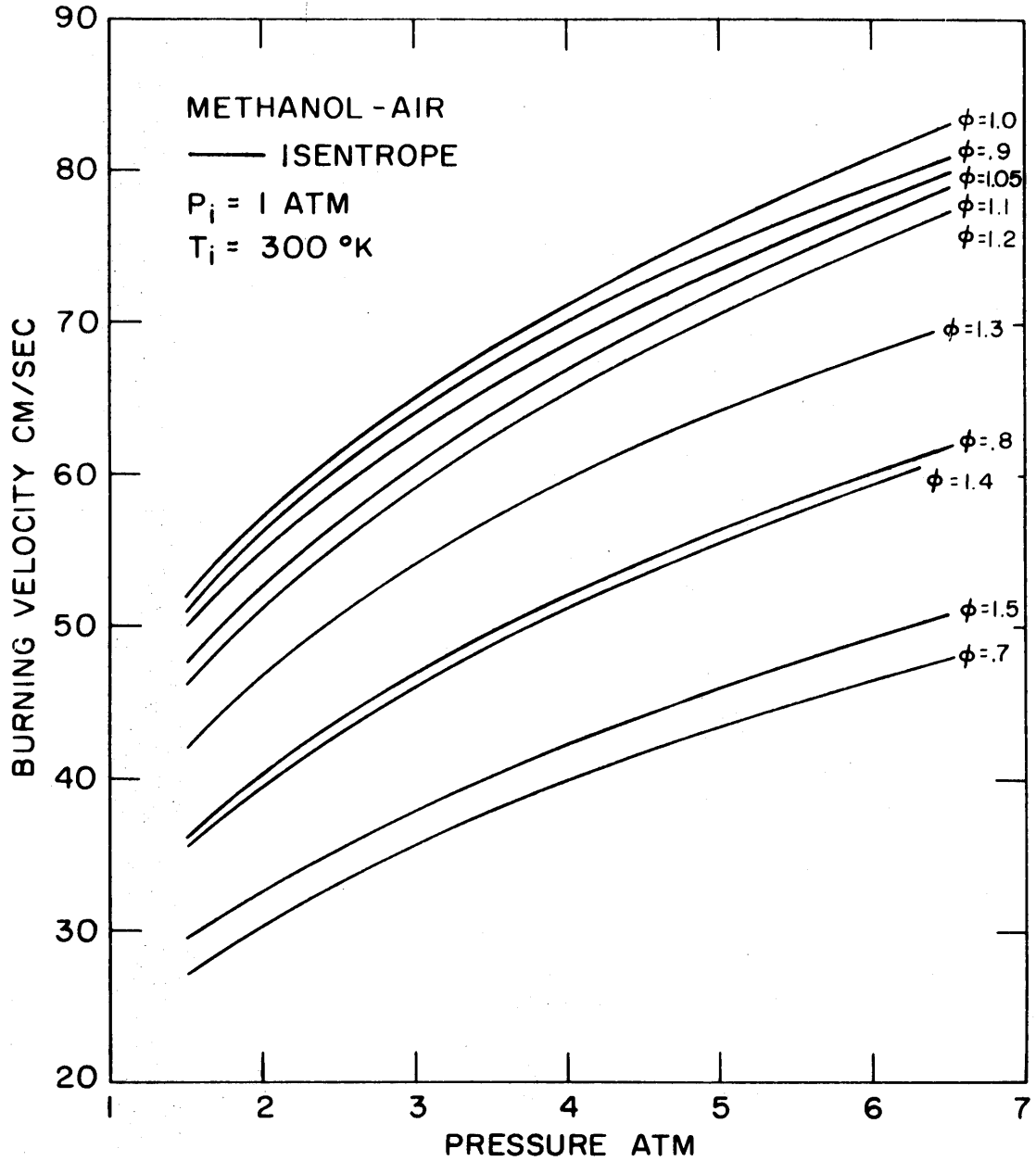


Figure 25: Burning Velocity for Isentropes of Methanol-Air Mixtures at Different Equivalence Ratio ϕ as a Function of Pressure with Initial Condition of $T_i = 300^\circ\text{k}$ and $P_i = 1 \text{ ATM}$.